AD-A232 419

SECUR

REPORT DOCUMENTATION PAGE

1a. REPORT SECURITY CLASSIFICATION	1b. RESTRICTIVE MARKINGS
2a. SECURITY CLASSIFICATION AUTHORITY	3. DISTRIBUTION/AVAILABILITY OF REPORT: Unlimited
2b. DECLASSIFICATION/DOWNGRADING SCHEDULE	
4. PERFORMING ORGANIZATION REPORT NUMBER(S)	5. MONITORING ORGANIZATION REPORT NUMBER(S): AFOSR-TR-
6a. NAME OF PERFORMING ORGANIZATION: University of Minnesota (6b. OFFICE SYMBOL (If applicable))	7a. NAME OF MONITORING ORGANIZATION: Same as 8a
6c. ADDRESS (City, State and ZIP Code): Physics - 116 Church St. S.E. Minneapolis, MN 55455	7b. ADDRESS (City, State and ZIP Code): " " SC
8a. NAME OF FUNDING/SPONSORING ORGANIZATION: AFOSR/NE (8b. OFFICE SYMBOL (If applicable))	9. PROCUREMENT INSTRUMENT IDENTIFICATION NUMBER: AFOSR-87-0345
8c. ADDRESS (City, State and ZIP Code): Bolling AFB Washington, D.C. 20332-6448	10. SOURCE OF FUNDING NOS.

PROGRAM ELEMENT NO.	PROJECT NO.	TASK NO.	WORK UNIT NO.
61102F	2306	C1	

11. TITLE (Include Security Classification): Epitaxial Iron Films

12. PERSONAL AUTHOR(S): E.D. Dahlberg - P.T. Cohen

13a. TYPE OF REPORT	13b. TIME COVERED	14. DATE OF REPORT (Yr., Mo., Day)	15. PAGE COUNT
Annual	FROM 12/15/89 TO 12/14/90	1/15/91	9

16. SUPPLEMENTARY NOTATION

17. COSATI CODES			18. SUBJECT TERMS (Continue on reverse if necessary and identify by block number)
FIELD	GROUP	SUB. GR.	

19. ABSTRACT (Continue on reverse if necessary and identify by block number)

This research involves studies of the magnetic properties of high quality thin and multilayered magnetic films. Both ultra high vacuum sputtering and molecular beam epitaxy techniques are utilized to prepare the films. Electrical transport is the primary probe to measure the magnetic properties of the films. Of special interest has been the determination of the temperature dependence of the magnetic anisotropy energies of epitaxial iron films and the transport properties of multilayers. In the anisotropy energy work the effects of interfacial strain and morphology have been the focus. In the transport effort has utilized multilayers of magnetic and nonmagnetic metals to study the interfacial scattering. The combination of a magnetic and nonmagnetic metal in this work facilitates the origin of the scattering by use of the anisotropic magnetoresistance.

20. DISTRIBUTION/AVAILABILITY OF ABSTRACT	21. ABSTRACT SECURITY CLASSIFICATION
UNCLASSIFIED/UNLIMITED ☐ SAME AS RPT. ☐ DTIC USERS ☐	UNCLASSIFIED

22a. NAME OF RESPONSIBLE INDIVIDUAL	22b. TELEPHONE NUMBER (Include Area Code)	22c. OFFICE SYMBOL
E.D. Dahlberg Weinstock K	(612) 624-3506	NC

DD FORM 1473, 83 APR EDITION OF 1 JAN 73 IS OBSOLETE.

DTIC ELECTE JAN 22 1991 D

ANNUAL REPORT FOR
AFOSR GRANT NO. AFOSR-89-0248

SUBMITTED TO
AIR FORCE OFFICE OF SCIENTIFIC RESEARCH
BOLLING AFB, DC 20332-6448

Grant Title: Epitaxial Iron Films

Starting Date: 12 Dec., 1989

Report Date: 15 Jan, 1991

Institution Name: University of Minnesota
Minneapolis, MN 55455

Co-Principal Investigators:
E.D. Dahlberg
School of Physics
& Astronomy
(612) 624-3506

P.I. Cohen
Dept. of Electrical
Engineering
(612) 625-5517

Business Office: Merlin Garlid
Asst. Director and Grant Administrator
Office of Research & Technology Transfer Administration
1919 University Avenue
St. Paul, MN 55104
(612) 624-2088

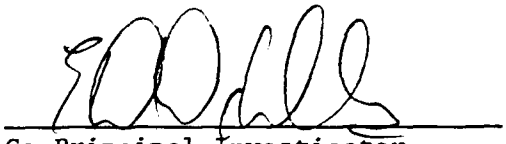

Co-Principal Investigator
E. D. Dahlberg
Professor

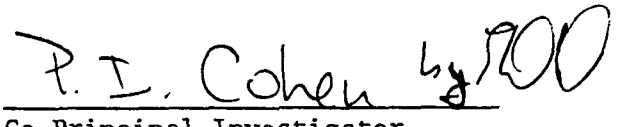

Co-Principal Investigator
P. I. Cohen
Professor

I. Statement of Work

This research program is directed at developing new models for a more fundamental understanding of magnetism and to investigate new magnetic phenomena such as the recent discovery of exchange coupled multilayers. The research focuses on the use of advanced thin film preparation techniques to prepare high quality multilayered and single thin films. Much of the research utilizes magneto-transport techniques to probe the magnetic properties of the magnetic films. The films are prepared by both ultra high vacuum sputtering and molecular beam epitaxy techniques. In particular, the magnetic phenomena being investigated include both a fundamental understanding of the spin-orbit coupling, the above mentioned exchange coupling, and a variety of interfacial effects. The interfacial effects include exchange coupling between ferromagnetic and antiferromagnetic films, electrical transport in multilayered magnetic systems, and the effects of interfacial morphology on magnetization pinning. The spin-orbit coupling effects are very important from both a basic science view and for magnetics applications. In terms of applications, the spin-orbit coupling determines the crystalline anisotropy energies and various other magnetically important quantities.

II. Magnetic Properties of Magnetic Multilayers and Thin Iron Films

As a mechanism of describing this research, we will list and discuss the publications which have been either published, submitted for publication, or are currently in draft form. The first three listings and reprints were included in the forecast report submitted in June, 1990. The fourth was submitted for publication and has since been published. These items are included for completeness in this annual report.

A. "A First Order Magnetic Field Induced Phase Transition in Epitaxial Iron Films Studied by Magnetoresistance," K.T. Riggs, E. Dan Dahlberg, and G. Prinz, Phys. Rev. B41, 7088 (1990).

This study focuses on the rotation of the saturation magnetization in the plane of the epitaxial iron films and utilizes the anisotropic magnetoresistance to follow the rotation of the magnetization in the presence of magnetic fields applied parallel to the plane of the films. As mentioned in A. above, the surface anisotropy energy in the (110) films is insufficient to rotate the magnetization out of the plane of the films. With the magnetization pinned in the plane of the film then the rotation of the magnetization in the plane of the films as a function of the magnitude and direction of a magnetic field applied in the plane of the film can be modeled as a first order transition. The easy way to understand this behavior is to consider two easy axes separated by a hard axis in the plane of the film. If the magnetization is required to rotate from one easy axis to the other by the application of a magnetic field, the applied magnetic field must be of sufficient strength that the magnetization can pass by the hard axis. Once this occurs the magnetization then abruptly (in a first order sense) makes the transition to the other easy axis. In the analysis of this behavior the uniaxial and fourth order anisotropy energies of the epitaxial films can be determined.

B. "Magnetic Domains in Epitaxial (100) Fe Thin Films," Jeffrey M. Florczak, P.J. Ryan, J.N. Kuznia, A.M. Wowchek, P.I. Cohen, R.M. White, G.A. Prinz, and E. Dan Dahlberg, Mat. Res. Soc. Symp. Proc. 151, 213 (1989).

This work shows how the surface morphology of the semiconductor substrate can influence the magnetic properties of the epitaxial magnetic films. It was found that the misfit dislocations which penetrate the surface of the InAs alloyed substrates can dominate the magnetic properties of the Fe films. The magnetics were investigated with both a magneto-optic magnetometer technique we developed (see below in other research) and with imaging Kerr microscopy. The most interesting feature of this research is the result that by correct preparation of the substrate the magnetization can be made almost isotropic in the plane of the film and controlled with modest applied magnetic fields (20 Oe).

C. Magnetic Anisotropy Constants of Epitaxial (110) Fe/GaAs Films From 77K to 293K Studied by Magneto-resistance," Daniel K. Lottis, G.A. Prinz, and E. Dan Dahlberg, Mat. Res. Soc. Symp. Proc. 151, 213 (1989).

Because the iron films are locked to the substrate the question arises as to the temperature dependence of various magnetic properties. In this paper we studied the temperature dependence of the anisotropy energies K_1 and K_u. A K_1 energy is also found in bulk iron whereas the K_u energy is unique to the epitaxial iron films. This paper determined that the K_u energy is consistent with a uniaxial strain arising from the growth of the metal film on the semiconductor at elevated temperatures. A comparison of the K_1 energy shows differences from that of bulk iron but the origin of the difference is uncertain.

D. "Detecting Two Magnetization Components by the Magneto-optical Kerr Effect," Jeffrey M. Florczak and E. Dan Dahlberg, published in the Jour. Appl. Phys. 67, 7520 (1990), (reprint enclosed)

A novel technique for detecting two orthogonal in-plane magnetization components was developed. This technique utilizes the magneto-optical Kerr effects to sense the two components. These components of magnetization are parallel and perpendicular to the plane of incidence of the light beam. The ability to sense two components, individually or simultaneously, is a result of the disparity in the longitudinal and transverse Kerr effects. Based on the Fresnel reflection coefficients of these two effects, an analysis is presented describing this dual component sensitivity. The physical conditions are given for simultaneous and individual detection of the two in-plane magnetization components. To substantiate this analysis, magneto-optical measurements are made on single crystal Fe films. The results are discussed in the context of dual component sensitivity. This procedure is useful for determining the magnetization process of thin films and as a probe to determine in plane preferential growth in polycrystalline films.

E. "Exchange effects in MBE grown iron films," Y-J Chen, D.K. Lottis, and E. Dan Dahlberg, J.N. Kuznia, A.M. Wowchak, and P.I. Cohen, accepted for publication in the J. Magn. and Magn. Mat. (preprint enclosed)

The films prepared in the MBE system are allowed to form a passivating oxide on the free surface. We discovered that this oxide orders antiferromagnetically at temperatures on the order of 200K. A comparison of the ordering temperature with the known oxides of iron allowed us to identify the oxide as FeO, which is the main result of this publication. The ordering of this oxide is manifest by its effects on the magnetic properties of the underlying iron films. The hysteresis loops of the iron films exhibit both an increase in the coercivity of the iron films and a shift in the hysteresis loops due to the exchange coupling to the antiferromagnetic oxide. Our investigation of this phenomena focused on the temperature dependence of both of these quantities. The research on the exchange coupling between the surface oxide and the iron film is potentially very exciting. At the present time a need for a detailed understanding of exchange coupling is necessary for several technologies from magneto-optic recording media to bias elements in thin film magnetometers. For this reason, it is anticipated that research on this phenomena will continue.

F. "Simultaneous in-plane Kerr effects in Fe/GaAs (110) thin films," J.M. Florczak, E. Dan Dahlberg, J.N. Kuznia, A.M. Wowchak, and P.I. Cohen, accepted for publication in the J. Magn. and Magn. Mat. (preprint enclosed)

In the case of the (110) grown films which have a hard or <111> direction separating the easy from intermediate directions, the magnetization process occurs via a discontinuous jump in the direction. The work on the use of magneto-optics to simultaneously measure the magnetization of two orthogonal components of the magnetization in a thin film (see D. above) was used to study how the magnetization in the epitaxial films evolves in the presence of an applied magnetic field. It is this technique which provided the data we used to model the effects of surface morphology on the magnetics of the

epitaxial films described earlier. In this publication, the technique allowed the observation of the discontinuous jump in the magnetization when realigning past the hard or (110) direction. In the previous work we were not able to monitor the magnetization continuously. This indicates the great utility of the MO technique.

G. "A model system for slow dynamics," D.K. Lottis, R.M. White, and E. Dan Dahlberg submitted for consideration of publication to Phys. Rev. Lett. (preprint enclosed)

The studies of the dynamics of the magnetization process in the thin iron films indicated a need to understand in greater detail the nucleation and magnetization process in magnetic systems. In this paper, we address how interactions in a magnetic system can give rise to slow dynamics. We used the dipolar coupling to provide the interaction in a planar system of spins. The remarkable result is that even when treated in the mean field limit, the system responds logarithmically in time. We were also able to show that the model replicates a stretched exponential over six decades in time. The most remarkable feature of the model is that it also predicts much of the behavior observed in the decay of the remanent magnetization observed in high temperature superconductors. In particular the quasilogarithmic decay and the nonmonotonic temperature dependence of the decay slope. In general, this paper indicates that interactions and not disorder may play a very important role in a number of physical systems from structural glasses to superconductors.

H. "Magnetization Reversal in (100) Fe Thin Films," Jeffery M. Florczak and E. Dan Dahlberg, to be submitted for publication to The Physical Review.

This publication is within a week or two of being ready for publication. It also utilizes the technique we developed using magneto-optics to provide a simultaneous measure of the magnetization in two orthogonal

directions in a magnetic film. This work focuses on (100) oriented iron films. These films differ from those we investigated earlier in that they do not possess all three primary three crystallographic directions in the film planes but instead only have the <100> and the <110> directions. The lack of the <111> direction completely alters the magnetization process. The (100) films appear to magnetize in a much more uniform manner. The data taken on these films was modeled with a uniform rotation of the magnetization direction. In the modeling, we were able to determine the anisotropy energies and, as expected, show that prior to a jump in the magnetization direction that the magnetization process is dominated by wall formation.

I. Near term publications: In addition to the research outlined above, we are currently studying superlattices of alternating layers of magnetic and nonmagnetic metals. This research appears to be providing insight to the transport properties of more complex systems than has been previously understood. Our use of the anisotropic magnetoresistance to determine the fraction of the scattering in the magnetic system has provided the key to resolve the scattering in the different layers. It is expected that there will be an increase in this area of research as our expertise increases. The initial samples investigated, prepared by Professor I.K. Schuller of UCSD and Argonne National Lab, were of Co and Ag. Since the completion of this initial work we have started a similar project using Fe and Cu for the metals. These samples also were prepared by Professor Schuller. We are currently preparing samples in our UHV sputtering system which was purchased with funds provided by the University of Minnesota and an AFOSR equipment grant (AFOSR-89-0138).

Another research area is the study of the spin-orbit interaction by the temperature dependence of the anisotropic magnetoresistance and anisotropy energies. In the films we have grown, it is anticipated that the largest effect of an altered iron lattice constant will be in those properties which depend up on the spin-orbit coupling. This has been shown already in iron films grown on GaAs substrates which compresses the iron lattice. This compression alters the spin-orbit coupling which determines the anisotropy energies in magnetic systems. In these films the small alteration of the

lattice constant is sufficient to rotate the easy axis from the (100) direction to the (110) direction. The spin-orbit coupling is the fundamental mechanism which determines the anisotropic magnetoresistance, the magnetoelastic coupling, the magneto-optic coupling, and provides a fundamental limit for the coercivity via the anisotropy energies. Although this one interaction is of fundamental and technical importance it is still not well understood theoretically. For this reason we are systematically studying many of the material properties which depend upon the spin-orbit coupling in order to provide the necessary information to develop a basic understanding and model of this interaction. This work was primarily being investigated by D. Lottis a PhD candidate. He has written his thesis and is currently on a Postdoctoral appointment with Dr. A. Fert in Orsay, France. It is anticipated that his thesis will be published a either a single major work on the above topics or if some require further efforts, it may result in several smaller Physical Review papers.

IV Personnel

A. Lottis,D.K., PhD Graduate in Physics (recipient of IBM predoctoral fellowship, 88-89 and University of Minnesota Dissertation Fellowship, 89-90), Currently on a postdoctoral appointment in Orsay with Dr. A. Fert.

B. Florczak,J.T., PhD Graduate Student in Physics (recipient of IBM predoctoral fellowship, 89-90).

C. Chen, Y.-J., PhD Graduate Student in Physics.

D. Tondra, M., Graduate Student in Physics.

E. Miller, B., Graduate Student in Physics.

F. Cleveland, J. was an undergraduate student in Physics, currently a fellowship graduate student in graduate school at U. C. Santa Barbara.

G. Truscott, A.T., Undergraduate Student in Physics.

H. Berg, M.A., Undergraduate Student in Physics.

I. Kaufmann, D., Undergraduate Student in Physics.

J. K. Sigsbee, K. Undergraduate Student in Physics.

K. Sankar, S., Undergraduate Student in Physics.

Detecting two magnetization components by the magneto-optical Kerr effect

J. M. Florczak and E. Dan Dahlberg
School of Physics and Astronomy, University of Minnesota, 116 Church St S.E., Minneapolis, Minnesota 55455

(Received 19 January 1990; accepted for publication 26 February 1990)

A novel technique for detecting two orthogonal in-plane magnetization components is presented. This technique utilizes the magneto-optical Kerr effects to sense the two components. These components of magnetization are parallel and perpendicular to the plane of incidence of the light beam. The ability to sense two components, individually or simultaneously, is a result of the disparity in the longitudinal and transverse Kerr effects. Based on the Fresnel reflection coefficients of these two effects, an analysis is presented describing this dual component sensitivity. The physical conditions are given for simultaneous and individual detection of the two in-plane magnetization components. To substantiate this analysis, magneto-optical measurements are made on single-crystal Fe films. The results are discussed in the context of dual component sensitivity.

I. INTRODUCTION

Conventional methods for obtaining magnetization loops, e.g., vibrating sample magnetometer (VSM), SQUID susceptometer, and BH loopers, are often constructed to detect only a single component of magnetization. A hysteresis curve from these single-component techniques is suitable for determining quantities such as the squareness, remanent magnetization, and the coercive field. These parameters are important in the characterization of magnetic materials. A hysteresis curve from these methods, however, provides only a limited amount of information about the reversal process. Additional information about the reversal can be obtained by rotating the sample in an applied field.[1] A more fundamental method for investigating the magnetization process entails measuring multiple components of the magnetization. Previous work along these lines has proved its utility, but the instruments are rather complex to construct.[2,3]

In this paper we present a novel method for detecting two in-plane magnetization components in ferromagnetic materials. This method utilizes the magneto-optical Kerr effect to sense the magnetization as a function of the applied field. The magneto-optical technique is not only simple to implement, but can be used to probe the magnetization in small regions of the sample. The dual sensitivity is based on the physical distinction between the transverse and longitudinal Kerr effects. The longitudinal effect is characterized by a rotation of the plane of polarization; the amount of rotation being proportional to the component of magnetization parallel to the plane of incidence. The transverse effect involves a change in the reflectivity of the light polarized parallel to the plane of incidence, not a rotation of the polarization. This change of reflectivity for the transverse effect depends upon the magnetization component perpendicular to the plane of incidence. These differences are described in Sec. II.

The difference in the two Kerr effects can be exploited by passing the reflected light through an analyzer. For a specific case, rotating the analyzer alters the dependence of the transmitted light on the two magnetization components. Hysteresis curves presented in the discussion section illustrate this connection between the analyzer orientation and the dual component sensitivity. For incident light polarized parallel to the plane of incidence, when the analyzer is near extinction (minimum light intensity), the intensity depends on the component of magnetization parallel to the plane of incidence. Rotating the analyzer 90° from extinction maximizes the response to the component of magnetization perpendicular to the plane of incidence. At angles intermediate between these two extremes, both components are simultaneously detected to varying degrees. It is this degree of control, coupled with the simplicity of the technique, that makes this method attractive in studies of magnetization processes.

The dual component detection can occur in both polycrystalline and single-crystal films. The data we present here represent what is possible with single-crystal films. In polycrystalline films, certain conditions must be present before two components can be detected. A laser "spot" comparable to the dimensions of a crystallite in a polycrystalline film can result in the detection of dual components. This would be useful in an investigation of interactions between crystallites during the magnetization process.

In the next section, the Fresnel reflection coefficients derived from a phenomenological theory of the magneto-optical Kerr effects are listed and examined. This is followed by an analysis describing the conditions for simultaneous or individual detection of the two magnetization components. A comparison of the theory and data for single-crystal films is then presented in Sec. IV. In Sec. V, some conclusions are discussed.

II. THEORY

The magneto-optical Kerr effects are categorized according to the geometry of the magnetization in relation to the plane of incidence and the film plane. The two Kerr

 0021-8979/90/127520-06$03.00

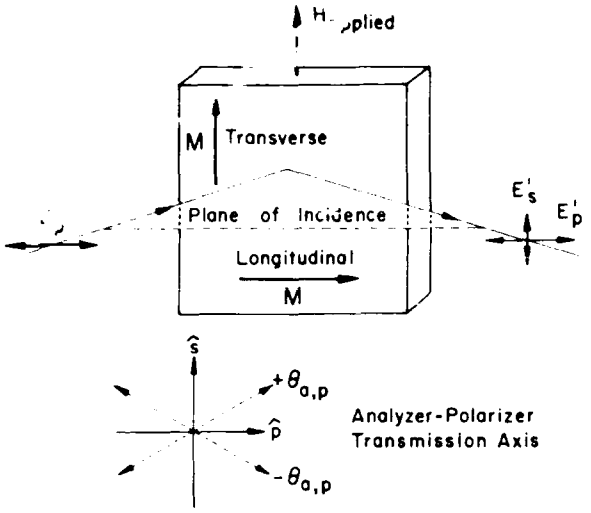

FIG. 1. Geometries for the transverse and longitudinal Kerr effects. The orientation of the analyzer and polarizer, $\theta_{a,p}$ are measured relative to the plane of incidence. A clockwise rotation, as viewed toward the light source, is defined as a negative angle while a counterclockwise rotation is a positive angle. The unit vectors, $\hat{s}$ and $\hat{p}$, denote directions perpendicular and parallel to the plane of incidence, respectively. The polarizations of the incident and reflected electric fields are also depicted.

effects involving in-plane magnetization are depicted in Fig. 1. In the transverse Kerr effect, the magnetization is perpendicular to the plane of incidence. In the longitudinal Kerr effect, the magnetization is parallel to the plane of incidence. The analysis of the dual component sensitivity is based on reflection coefficients derived from a phenomenological model of the Kerr effects.[4-7] In this model, the Kerr effect is described by a dielectric tensor with off diagonal elements. These elements of the dielectric tensor depend upon the Voigt magneto-optical parameter Q.[7] Residing in this parameter is the interaction of the electromagnetic field with the magnetic electrons. By virtue of this, Q is proportional to the magnetization in the ferromagnet. The reflection coefficients listed here for the transverse and longitudinal Kerr effects are only approximate. Terms higher than order Q are neglected. Typically $|Q|$ is small, but there are exceptions.[8] In addition, the film thickness is large compared to the skin depth of the light so that the substrate-film interface can be neglected.

Starting with the transverse Kerr effect, the Frensel reflection coefficients connecting the incident and reflected electric fields of given polarizations are

$$r^t_{pp} = \begin{pmatrix} n\beta & \beta' \\ n\beta & +\beta' \end{pmatrix} \left(1 + \frac{\kappa_2 \sin 2\theta}{n^3 (n^2 \cos^2 \theta - 1) + \sin^2 \theta} \right), \tag{1}$$

$$r^t_{ss} = (\beta - n\beta')/(\beta + n\beta'), \tag{2}$$

$$r^t_{ps} = r^t_{sp} = 0. \tag{3}$$

In the above, the quantity r^t_{ps}, for example, is the coefficient for the transverse effect relating the incident s wave to the reflected p wave. The s and p refer to light that is polarized perpendicular and parallel to the plane of incidence, respectively. The angle of incidence measured from the sample normal is θ, n is the index of refraction of the material, $\kappa_2 = in^2 Q$ is the off diagonal element of the relative permittivity tensor, $\beta = \cos\theta$, and $\beta' = [1 - (\sin^2\theta)/n^2]^{1/2}$. From these Frensel coefficients, one should note that the reflected light does not undergo a rotation. The only magnetization-dependent quantity, in this case, is the reflection coefficient connecting the incident and reflected p polarized light. Practically speaking, this implies that hysteresis loops can be taken without a polarizer or analyzer when the transverse effect is present.

The Fresnel reflection coefficients for the longitudinal Kerr effect are

$$r^l_{pp} = (n\beta - \beta')/(n\beta + \beta'), \tag{4}$$

$$r^l_{ss} = (\beta - n\beta')/(\beta + n\beta'), \tag{5}$$

$$r^l_{ps} = -r^l_{sp} = \frac{\gamma\beta\kappa_2}{n^2\beta'(n\beta + \beta')(\beta + n\beta')}, \tag{6}$$

where the superscript l refers to longitudinal and $\gamma = \sin\theta$. The other terms are defined earlier in connection with Eq. (1). The above coefficients describe a rotation of the incident polarization by the presence of the off diagonal terms, r^l_{sp} and r^l_{ps}. In contrast to the transverse Kerr effect, the diagonal terms here do not depend upon the magnetization. A final note about all the coefficients in the limit that $Q \to 0$, implying that the material is no longer magnetic, the distinction between the two geometries vanishes, and the reflection coefficients reduce to those of normal metallic reflection.

Generalizing to the case of two Kerr effects, consider plane polarized light incident upon a ferromagnetic sample having both longitudinal and transverse Kerr geometries (see Fig. 1.). As an example, consider the film to be in a single domain state with the in-plane magnetization at an angle of 45° relative to the plane of incidence. This magnetization vector can be decomposed into components parallel and perpendicular to the plane of incidence. If the film is exposed to an applied field, the magnetization will alter its orientation to minimize the energy of the film. As the magnetization changes so will the Frensel coefficients describing the reflection. Experimentally, the reflected p wave will alter in amplitude due to the component of magnetization perpendicular to the plane of incidence. The variation of the s-wave component in the reflected light is a result of the magnetization component parallel to the plane of incidence. By passing the light through an analyzer and rotating it so that either the s wave or p wave is transmitted, thereby blocking the other orthogonal component, allows selective detection of either component.

The remaining analysis focuses on the relation between the intensity detected by a photodiode and the polarizer-analyzer angles. First, we denote the transmission axis of the polarizer as θ_p and the analyzer as θ_a. For an observer looking toward the photon source, the angles are defined to be positive (negative) for a counterclockwise (clockwise) rotation from the plane of incidence (see Fig. 1).

The electric field after transmission through the polarizer has the vector form

$$\mathbf{E} = E_i \cos\theta_p \hat{\mathbf{p}} + E_0 \sin\theta_p \hat{\mathbf{s}}. \tag{7}$$

In this expression $\hat{\mathbf{p}}$ denotes the unit vector parallel to the plane of incidence and $\hat{\mathbf{s}}$ denotes the unit vector perpendicular to the plane of incidence. This light is incident upon the ferromagnetic film. The interaction of the light with the multiple Kerr effects, and the subsequent reflection, can be expressed in terms of a general scattering matrix.[7] For two in-plane magnetization components this matrix is

$$S^{\text{total}} = m_t^2 S^t(Q/m_t) + m_l^2 S^l(Q/m_l), \tag{8}$$

where $m_t = M_t/M_s$ and $m_l = M_l/M_s$. Here M_t is the component of magnetization perpendicular to the plane of incidence, M_l is the component of magnetization parallel to the plane of incidence, M_s is the saturation magnetization, and the scattering matrices for the transverse and longitudinal Kerr effects are $S^t(Q/m_t)$ and $S^l(Q/m_l)$, respectively. These scattering matrices for the transverse and longitudinal Kerr effects can be reduced to matrices describing only the reflection at one interface. For the case of the transverse effect, the matrix is

$$S^t(Q/m_t) = \begin{pmatrix} r^t_{pp} & r^t_{ps} \\ r^t_{sp} & r^t_{ss} \end{pmatrix}. \tag{9}$$

The term in parentheses, Q/m_t, denotes that wherever a Q appears in the Frensel coefficients of the transverse Kerr effect, Q/m_t should replace that Q. Since the magnetization is restricted to be in-plane, $m_l^2 + m_t^2 = 1$. Using this result in relation (8), the electric field after reflection from the ferromagnetic sample is

$$\begin{aligned} E'_p &= (m_l^2 r^l_{pp} + m_t^2 r^l_{pp}) E_0 \cos\theta_p + m_t^2 r^l_{ps} E_0 \sin\theta_p, \\ E'_s &= m_t^2 r^l_{sp} E_0 \cos\theta_p + r^l_{ss} E_0 \sin\theta_p. \end{aligned} \tag{10}$$

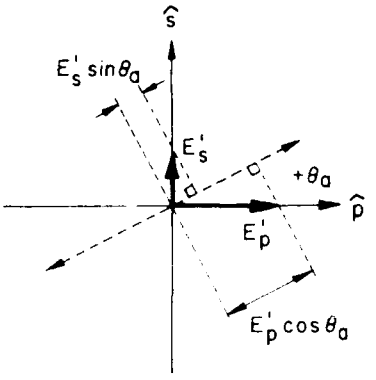

FIG. 2. Graphical representation of the decomposition of the reflected electric field into components parallel and perpendicular to the analyzer transmission axis. The analyzer transmission axis is rotated $+\theta_a$ from the plane of incidence. The components of the reflected light which pass through the analyzer are $E'_s \sin\theta_a$ and $E'_p \cos\theta_a$.

This reflected light is sent to the analyzer where only the component parallel to the analyzer transmission axis will pass. Figure 2 shows the decomposition of this electric field into components parallel and perpendicular to the transmission axis. This transmitted component is subsequently sensed by a photodiode. In terms of the reflected electric field, the transmitted light is

$$E_t = E'_s \sin\theta_a + E'_p \cos\theta_a. \tag{11}$$

Substituting Equations (10) into Eq. (11) and simplifying the result, the electric field parallel to the analyzer transmission axis is

$$\begin{aligned} E_t = E_0[&(m_l^2 r^l_{pp} + m_t^2 r^l_{pp})\cos\theta_p \cos\theta_a + m_t^2 r^l_{ps} \sin(\theta_p \\ &- \theta_a) + r^l_{ss} \sin\theta_p \sin\theta_a]. \end{aligned} \tag{12}$$

The output current from a photodiode sensing this light is proportional to the modulus squared of Eq. (12). Thus, the resulting expression for the detected signal, normalized to the incident intensity, is

$$\begin{aligned} I/I_0 = [&|m_l^2 r^l_{pp} + m_t^2 r^l_{pp}|^2 \cos^2\theta_p \cos^2\theta_a + |m_t^2 r^l_{ps}|^2 \sin^2(\theta_p - \theta_a) + |r^l_{ss}|^2 \sin^2\theta_p \sin^2\theta_a + [(m_l^2 r^l_{pp} + m_t^2 r^l_{pp}) m_t^2 r^{l*}_{ps} \\ &+ \text{c.c.}] \cos\theta_p \cos\theta_a \sin(\theta_p - \theta_a) + [(m_l^2 r^l_{pp} + m_t^2 r^l_{pp}) r^{l*}_{ss} + \text{c.c.}] \sin\theta_p \sin\theta_a \cos\theta_p \cos\theta_a \\ &+ [r^l_{ss} m_t^2 r^{l*}_{ps} + \text{c.c.}] \sin\theta_p \sin\theta_a \sin(\theta_p - \theta_a)]. \end{aligned} \tag{13}$$

III. SINGLE- AND DUAL-COMPONENT DETECTION

In the experimental setup, due to the use of a polarized laser, it is convenient to fix the incident polarization and vary the analyzer angle. In light of this, it is desirable to find simplifying cases of Eq. (13) for fixed polarizer angles θ_p. Three cases are found that reduce expression (13). For two of these, only a single magnetization component is detected. This occurs when $\theta_p = 90°$ (s polarized) and also when $\theta_p = \theta_a$. When $\theta_p = 90°$, the intensity is sensitive to variations of the component parallel to the plane of incidence. When $\theta_p = \theta_a$, the intensity depends upon the component perpendicular to the plane of incidence. For the situation in which $\theta_p = \theta_a = 90°$, a possibility that apparently satisfies both of the above cases, the intensity is independent of the magnetization and therefore neither is observed. The third simplifying case, $\theta_p = 0°$ (light polarized parallel to the plane of incidence), results in the detection of two magnetization components. Because of the simplicity and importance of this sensitivity to both magnetization components, the remaining analysis concentrates on this arrangement.

Substituting $\theta_p = 0°$ in Eq. (13), the expression simplifies to

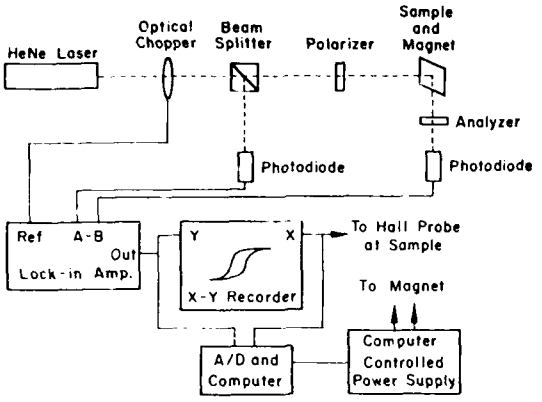

FIG. 3. Block diagram of the hysteresis loop tracer. The system is enclosed in a thermally stabilized enclosure to minimize mode sweeping of the 2-mW HeNe laser.

$$I/I_0 = |m_l^2 r_{pp}^l + m_t^2 r_{pp}^t|^2 \cos^2\theta_a + |m_l^2 r_{ps}^l|^2 \sin^2\theta_a - [(m_l^2 r_{pp}^l + m_t^2 r_{pp}^t) m_l^2 r_{ps}^{l*} + \text{c.c.}] \cos\theta_a \sin\theta_a. \quad (14)$$

This relation predicts that for $\theta_a \simeq 0°$ the intensity is specifically sensitive to changes in the magnetization component perpendicular to the plane of incidence. This is easy to see by noting that relations (1) and (4) combine in $m_l^2 r_{pp}^l + m_t^2 r_{pp}^t$ to give a sum of a nonmagnetic term and a term proportional to QM_t/M_s. For $\theta_a \simeq 90°$ the intensity depends primarily on the component parallel to the plane of incidence. This component appears as QM_l/M_s and $|Q|^2 M_l M_t / M_s^2$ in the $\sin\theta_a \cos\theta_a$ term and as $|Q|^2 M_l^2/M_s^2$ in the $\sin^2\theta_a$ term. The terms quadratic in Q are small in comparison to the linear terms since $|Q|$ is taken to be small. At analyzer angles between these extremes, the intensity depends upon both components. The degree of sensitivity to each component can be controlled by rotating the analyzer to the required angle. An important prediction of Eq. (14) concerns the last term on the right. The sine function is odd in the angle θ_a hence, the $\sin\theta_a \cos\theta_a$ term can change sign depending if the analyzer is at $-\theta_a$ or $+\theta_a$. The distinction between positive and negative is only real for angles $0° < |\theta_a| < 90°$. The significance of the $\sin\theta_a \cos\theta_a$ term can be deduced from the data by comparing the $+\theta_a$ and $-\theta_a$ hysteresis loops.

IV. EXPERIMENTAL DETAILS

Figure 3 is a block diagram of the hysteresis loop tracer. The system is maintained in a thermally stabilized box to minimize mode sweeping of the HeNe laser.[9] The light is split into two beams, one is directed to the sample and the other is sent to a reference photodiode. The light incident upon the sample is polarized in the plane of incidence, $\theta_p = 0°$, and the angle of incidence is maintained at 60° in all the data. The intensity detected by the lock-in amplifier is $\Delta I = I(M) - I_{\text{ref}}$. Here $I(M)$ is the signal from the sample and I_{ref} is the intensity from the reference beam. The voltage from the reference photodiode is adjusted via a voltage divider so that ΔI is zero when the sample is demagnetized. This procedure is used to minimize the magnetization-independent intensity (normal metallic reflection from the ferromagnet) when the analyzer is adjusted from extinction.

The analyzer and polarizer are both Glan–Thompson prism polarizers which have an extinction ratio of 1×10^{-6}.[10] This high extinction ratio is important for separating the s and p polarized light. The plane of incidence is determined by adjusting the polarizer and analyzer for minimum intensity when the film is demagnetized. Near extinction, the intensity depends quadratically on the polarizer or analyzer angle so that the plane of incidence can be determined fairly accurately.[11]

The film is mounted on a rotatable sample stage; this allows the applied field to be oriented at any particular angle relative to the crystalline axes of single-crystal films. The external field is applied in the plane of the film, and perpendicular to the plane of incidence. The intensity data can be stored digitally or with an X-Y recorder for later analysis. The hysteresis curves are typically acquired in less than 2 min and at room temperature.

V. RESULTS AND DISCUSSION

To support the above analysis, measurements were made on single—crystal Fe films epitaxially grown on (100) GaAs. The preparation of these samples have been previously discussed.[12] The epitaxial growth of Fe on the (100) plane of GaAs constrains the Fe to form a (100) plane. In the (100) plane of Fe there are two magnetically easy ⟨100⟩ axes and two magnetically intermediate ⟨110⟩ axes. The remaining discussion focuses on the hysteresis curves taken with the applied field nearly parallel to a magnetically intermediate ⟨110⟩ axis. It should be emphasized that all the data are taken with the same orientation of the applied field, only the analyzer angle is varied.

This first example centers on the measurement of the magnetization component parallel to the applied field. The previous analysis indicates that for $\theta_a \simeq 0°$ any intensity change is due to the component of magnetization perpendicular to the plane of incidence. The hysteresis curve for $\theta_a = 0°$ is depicted in Fig. 4(a). With reference to Fig. 1, in this experimental setup the component of magnetization perpendicular to the plane of incidence is also parallel to the applied field. As the field is increased this component grows in a manner indicative of coherent rotation. When the field surpasses approximately $2K_1/M_s \simeq 550$ Oe (bulk Fe constants), the magnetization saturates in the direction of the applied field. Hysteresis curves obtained from a SQUID susceptometer with the field parallel to the magnetically intermediate axis of this sample are similar to this curve. Thus, for this analyzer orientation this method could be directly compared to other single-component measurement techniques.

The second example corresponds to sensing the magnetization component perpendicular to the applied field. Figure 4(b) depicts the hysteresis curve for $\theta_a \simeq 90°$. At this analyzer orientation the intensity variations are a result of the magnetization component parallel to the plane

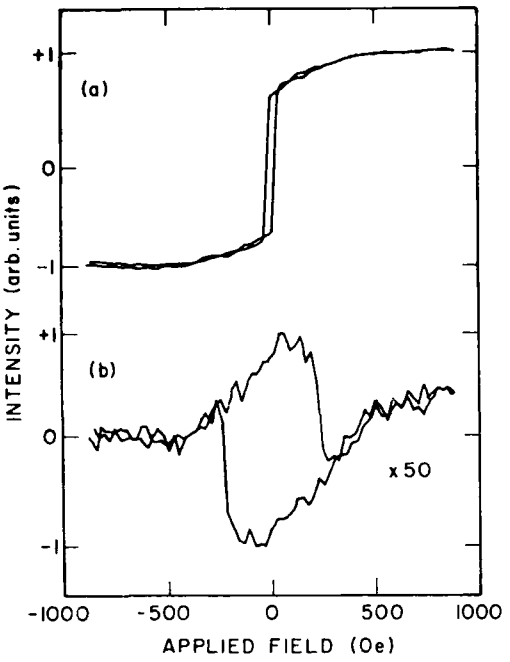

FIG. 4. Hysteresis curves for (a) $\theta_a = 0°$ and (b) $\theta_a = -85°$ when the applied field is along a ⟨110⟩ magnetically intermediate axis of the crystal. The $\theta_a = 0°$ data is scaled to bring the $+M_s$ and $-M_s$ saturation states to arbitrary intensities of $+1$ and -1, respectively. The scaling of (b) and the curves in Fig. 5. are relative to this $\theta_a = 0°$ curve.

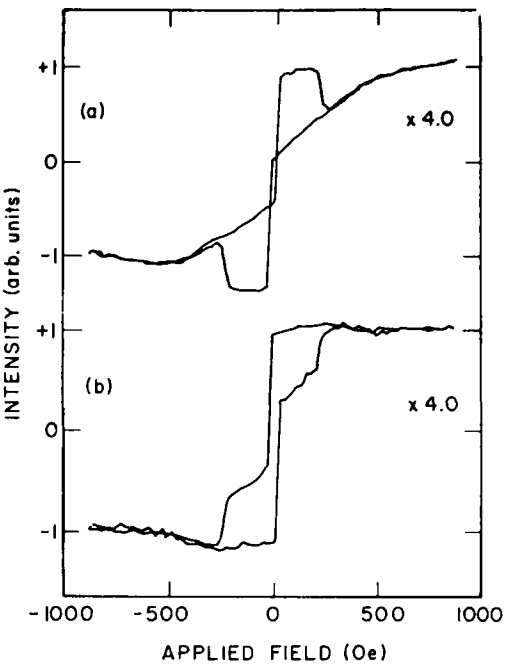

FIG. 5. Hysteresis curves for the same applied field orientations as in Fig. 5 but with analyzer angles of (a) $\theta_a = -60°$ and (b) $\theta_a = +60°$. The intensity variation here depends upon both magnetization components. The first transition occurs at a field of 20 Oe while the second transition occurs at a field of 250 Oe.

of incidence. By similar reasoning as before, the magnetization component parallel to the plane of incidence is also perpendicular to the applied field. As the field is increased and the magnetization gradually increases in the direction of the applied field, the component perpendicular to the applied field vanishes. This is true regardless of the polarity of the applied field. This explains why the light intensity is so similar at the two saturated states. At low fields near 0 Oe, due to the orientation of the ⟨100⟩ easy axes, the magnetization is angled 45° from the plane of incidence. This maximizes the component perpendicular to the applied field for this sample. Hence, the intensity values have a maximum difference near 0 Oe between the positive and negative magnetization directions. The reversal field for this magnetization component is rather large compared to the component parallel to the applied field, 250 versus 20 Oe. This disparity is a result of the particular magnetization process occurring in the film.[13] With this orientation of the analyzer, $\theta_a \simeq 90°$, it is possible to determine the changes of the magnetization component parallel to the plane of incidence.

In this last example, we examine the magnetization loops resulting from the detection of two magnetization components. The simultaneous detection of two magnetization components is predicted to occur at θ_a angles between 0° and 90°. Depicted in Fig. 5 are hysteresis curves for analyzer angles of $+60°$ and $-60°$. A comparison of the positive and negative analyzer angles, $+\theta_a$ and $-\theta_a$, determines those regions where the $\sin\theta_a \cos\theta_a$ term of relation (14) is of importance. For this sample, the sign dependent term is significant for fields less than about 550 Oe. The simultaneous detection of both in-plane components is inferred by the two transitions appearing in these data. The first transition, relative to 0 Oe, occurs at 20 Oe and the second at 250 Oe. These reversal fields are similar to the reversal fields observed in Fig. 4 for the components parallel and perpendicular to the applied field, respectively. The overshoots and undershoots in these curves are a result of the particular mixing of the two Kerr effects and are further evidence of the dual-component detection.[13]

We now turn to the question if this technique can be used on polycrystalline films. The above analysis assumes the laser illuminates a single crystal. The results are still valid if the area illuminated by the laser is a single crystallite of a polycrystalline film or a polycrystalline film that has an in-plane preferred growth direction. In an isotropic polycrystalline film, if the area illuminated contains many crystallites, a superposition of the individual magnetization vectors in each crystallite results in a magnetization vector parallel to the applied field. Hence, for a large laser spot two-component detection would not be expected. This was confirmed by magneto-optical measurements taken of polycrystalline Fe films. The shape of the hysteresis curve did not depend on the analyzer angle as in the single-crystal films.

For the case of a polycrystalline film with an in-plane preferred growth direction, many of the crystallites will, to some degree, have their crystalline axes aligned. A superposition of the magnetization vectors in this case can result in a net magnetization with a component perpendicular to the applied field. The detection of two components in this

situation would be similar to that of single-crystal films. This is where these measurements could serve a dual purpose by detecting any in-plane anisotropy of polycrystalline films due to growth conditions or substrate texture.

VI. CONCLUSIONS

This paper presents a novel technique, based on the magneto-optical Kerr effects, for monitoring two components of the magnetization as a function of the applied field. For the particular situation when the incident light is polarized in the scattering plane, a rotation of the analyzer to 90° or 0° detects magnetization components parallel or perpendicular to the plane of incidence. At angles intermediate between these extremes both components are simultaneously sensed to varying degrees. With suitable modifications of the beam diameter of the laser or anisotropic growth conditions for films, this technique can be used on polycrystalline films.

The in-plane magnetization components can also be detected simultaneously but separately. This is accomplished by adding a beam splitter and a second analyzer/photodiode combination to the reflected light. The analyzers are adjusted so that one senses the component parallel to the plane of incidence and the other detects the component perpendicular to the plane of incidence. In this way, one does not rotate the analyzer to detect the individual components.

ACKNOWLEDGMENTS

We wish to express our gratitude to the AFOSR for their support in this research under Grant No. AF/AFOSR-89-0248. One of us, J. Florczak, would like to thank IBM for their support under an IBM fellowship. A special thanks to J. N. Kuznia in the E. E. Department at the University of Minnesota and M. P. Dugas at Advanced Research Corp. for providing the samples used in this study.

[1] U. Admon, M. P. Dariel, E. Grunbaum, and J. C. Lodder, J. Appl. Phys. **66**, 316 (1989).
[2] E. M. Bradley and M. Prutton, J. Electron. Control **6**, 81 (1959).
[3] C. D. Olson and A. V. Pohm, J. Appl. Phys. **29**, 274 (1958).
[4] J. H. Judy, Proceedings, Conference on Advances in Magnetic Recording, N.Y. Acad. of Science **189**, 239 (1972).
[5] M. J. Freiser, IEEE Trans. **MAG-4**, 152 (1968).
[6] R. P. Hunt, J. Appl. Phys. **38**, 1652 (1966).
[7] C. C. Robinson, J. Opt. Soc. Am. **53**, 681 (1963).
[8] H. Schewe and H. Hoffmann, Physica B **89**, 59 (1977).
[9] A. D. White, Laser Focus/Electro-Optics, August (1985).
[10] Karl Lambrecht Corp., Chicago, Ill.
[11] B. D. Cahan, R.F. Spanier, Surf. Sci. **16**, 166 (1969).
[12] D. K. Lottis, J. Florczak, and E. Dan Dahlberg, J. Appl. Phys. **63**, 3662 (1988).
[13] J. M. Florczak and E. Dan Dahlberg (to be published).

EXCHANGE EFFECTS IN MBE GROWN IRON FILMS

Youjun Chen, Daniel K. Lottis, and E. Dan Dahlberg
School of Physics and Astronomy

J. N. Kuznia, A. M. Wowchak and P. I. Cohen
4-178 Electrical Engineering and Computer Science Bldg.

University of Minnesota
Minneapolis, MN 55455

ABSTRACT:

The magnetic properties of molecular beam epitaxy iron films grown on (001) GaAs substrates were studied using a SQUID magnetometer. In uncapped films, where there is an oxidized iron layer on top of the film, the M-H loops shift from being symmetric about the origin when the film is cooled in applied fields to temperatures below 100K. The observed behavior is attributed to a unidirectional exchange anisotropy generated by the antiferromagnetic ordering of the oxidized iron surface. By comparing the magnitude of the exchange coupling observed in these films with that observed in the Co-CoO system, the oxide which forms on the iron surface is most likely FeO. In addition, we have studied the magnetic training effect or the effect of cycling through the hysteresis loops at fixed temperatures. It is noted that the temperature dependence of the measured exchange coupling is different from that which is usually reported. The reason for this difference is unknown.

PACS number: 75.30.Et, 75.50.Bb, 75.70.-i.

Introduction

Exchange coupled ferromagnetic (F) and antiferromagnetic systems demonstrate a shifted hysteresis loop when the systems are cooled in a magnetic field to below the Neel temperature of the antiferromagnetic (AF) layer.[1] Another feature of this phenomena is that there is a magnetic training effect,[2] i.e., at a fixed temperature, the magnitude of the observed effect depends upon the magnetic history of the sample at that temperature. Although many features of this effect are not well understood, we have used a comparison of the magnitude of the shift observed in epitaxed iron films to that in Co-CoO exchange coupling to identify the oxide which forms on the epitaxed iron film surfaces as FeO. In addition, the temperature dependence of the shift and the coercivity, and its thickness dependence are reported.

Experimental Details and Results

The iron films used in this study were grown by molecular beam epitaxy on (001) GaAs substrates at 200 C. After film growth, the normal procedure was to move the film to the introduction chamber after the film had cooled. This chamber was then filled with air which resulted in the formation of a self-passivating iron oxide layer, removing

about 1.5 nm thick of Fe.[3] As a control, one sample was covered with amorphous GaAs in the growth chamber prior to its exposure to air, prohibiting the iron oxide growth.

The magnetic measurements were taken following a number of different magnetic field-temperature paths. For most of the data, a magnetic field on the order of 1000 Oe was applied in the plane of the sample along a magnetically easy axes with the sample at room temperature, cooled to a lower temperature and a hysteresis loop was measured. Next the sample was warmed to a higher temperature and another hysteresis loop was measured. Other data were accumulated by always warming the sample to room temperature, reapplying the magnetic field and then cooling to another temperature. In addition, for measurements made when the samples were cooled in zero applied field, the samples were always demagnetized prior to cooling.

The main experimental observation in the data is a shift in the hysteresis loop for the iron oxide covered films cooled in the presence of an applied magnetic field as illustrated in fig.1. This shift results from a coupling between the ferromagnetic iron film and the antiferromagnetic iron oxide which forms on the free surface of the iron films. The reason to attribute the antiferromagnetism to the oxide is that the data taken on the sample which was prepared with the GaAs protective overcoat, therefore lacking an iron oxide, did not exhibit

any features indicative of exchange coupling at any temperature.

For all the field cooled samples, a measurable shift in the hysteresis loops occurred starting at temperatures on the order of 100K or below. The data were quantified in the following manner, the shift from the origin for the hysteresis loops was defined as the exchange field, H_e and one-half the total width of the loops was defined as the coercive field, H_c. For all the data shown here, the samples were cooled in a magnetic field to a low temperature, usually on the order of 5K and then the hysteresis loops were measured warming the sample and stabilizing the temperature for each loop. The fact that there is a training effect, which will be discussed next, introduces some error in the data accumulated in this manner, however by using both techniques described above, it was determined that the error is minimal. The data showing the temperature dependence of H_e and H_c for the four samples measured which exhibit this behavior are shown in figures 2 and 3.

The magnetic training effect refers to the gradual reduction in the exchange field and coercivity with the number of hysteresis loop cycles at a fixed temperature. Behavior of this type has been previously reported[4] with attempts at a theoretical understanding[2], however at the

present there does not appear to be a wholly satisfactory model for this effect. One feature of the present work is there appears to be a strong thickness dependence to the magnitude of the training effect. Only two of the four samples were studied in depth for the magnetic training effect but of these two samples, the training effect was considerably larger in the thinner sample. As an example, at 5K, the reduction in H_e after one hysteresis cycle was 45% for a sample 2.0 nm thick, and only 15% for a sample 6.0 nm thick.

Discussion of Results

Simple considerations[2] show that the loop shift and the ferromagnetic-antiferromagnetic exchange constant are related by the following expression,

$$t_F H_e M = nJ_K, \qquad (1)$$

where t_F is the thickness of the ferromagnetic layer, H_e is the loop shift, M is the magnetization of the ferromagnetic layer, n is the areal density of spins at the interface, and J_K is the exchange constant between the F-AF spins per unit interface area. From (1), the loop shift is inversely proportional to the thickness of the ferromagnetic layer. This is consistent with the data which are shown in fig. 4

which is a plot of the H_e's measured at 5K versus the inverse of the thickness for the four films studied. Using expression (1), the magnitude of the exchange coupling constant, J_K, between the F and AF spins across the interface was found to be 9.3×10^{-17}erg at a temperature of 5K. For comparison, in the Co-CoO system the zero temperature value of J_K was found to be 5.59×10^{-16}ergs.[5]

It is interesting to speculate on the magnitude of the coupling energy one should expect to observe. Although it is difficult to determine the interface exchange, one might expect it to be related to the exchange energy of the metal and the oxide. Both Co and Fe have comparable exchange energies so one might expect the above energy differences to be associated with the oxide. In the case of CoO, the Neel temperature is on the order of room temperature. Postulating that FeO is the oxide which forms on the iron films, it has a Neel temperature on the order of 200K. The ratio of the two Neel temperatures would indicate that the value expected for the Fe-FeO system should be on the order of 3.8×10^{-16}ergs which is in reasonable agreement with the experimental result given that the above argument does not include any differences in the coupling of the metals to the oxides.

There has been a report[6] that FeO forms on iron films in an oxygen environment. This same study also stated that

for iron oxides grown in an ambient environment, the oxide which forms is probably either Fe_3O_4 or γ-Fe_2O_3. We cannot positively rule out the possibility of either one of these last two oxides being present, however, the effect which is observed must have its origin in an antiferromagnetic material. It is certainly possible that all three species are present which might also explain other features of the data which are discussed below.

It is usual for the H_e to be linear in temperature.[2] However, it is clear from fig. 1 that this is not the case for the samples reported here. This nonlinear decrease in H_e might come from the temperature dependence of the anisotropy in the antiferromagnetic iron oxide. In the above, we have assumed that the antiferromagnetic lattice is locked or is not free to rotate with the iron. If this is not the case then the H_e which would be measured would reflect the antiferromagnet anisotropy energy and not the exchange coupling. As an example of this, in the Ni-NiO system, there is no effect of the antiferromagnetic ordering of the NiO on the hysteresis loops because of the small value of the anisotropy energy of NiO.[7] This might be a possible explanation for the temperature dependence of H_e and is also a possible explanation why the J_K measured is low compared to the Co-CoO system. On the negative side of this argument, if this is the case then one might expect the

training effect to be larger than normal. This possibility was not fully investigated, however, at the lowest temperatures the training effect was comparable to that observed in other systems.[4]

Summary

A study of the effects of exchange coupling in ferromagnetic iron-antiferromagnetic iron oxide has been made. As expected, the magnitude of the observed shift in the hysteresis loops is proportional to 1/t of the iron films. By comparing the magnitude of the interfacial energy in the Fe-Fe oxide films to that observed previously in Co-CoO interfaces, the Fe oxide has been identified as FeO. The temperature dependence of the exchange field is different from that usually observed. This may be due to the fact that the FeO has a Neel temperature of 200K and therefore over the temperature range investigated, the anisotropy energy of the FeO may be changing.

Acknowledgements

The authors would like to thank the AFOSR for support of this research under grant number AFOSR-89-0248

REFERENCES:

1. W. H. Meiklejohn and C. P. Bean, Phys. Rev. 102, 1413 (1956).
2. A. P. Malozemoff, J. Appl. Phys. 63, 3874 (1988).
3. M. Rubinstein, F. J. Rachford, W. W. Fuller, and G. A. Prinz, Phys. Rev. B. 37, 8689 (1988).
4. C. Schlenker, S. S. P. Parkin, J. C. Scott, and K. Howard, J. Magn. Magn. Mater. 54-57, 801 (1986).
5. W. H. Meiklejohn and C. P. Bean, Phys. Rev. 105, 904 (1957). The coupling constant was calculated by using the loop shift extrapolated at 0K.
6. A. J. Melmed and J. J. Carroll, J. Vac. Sci. Technol. 10, 164 (1973).
7. A. Yelon, Progr. Thin Films 6, 205 (1971).

Figure Captions:

1. The measured shifted hysteresis loop at 5K for a 60A thick film after cooling in a 1000 Oe applied field.

2. The measured dependence of the loop shifts or H_e on temperature. The symbols plus +, block ■, cross ×, and square □ correspond to sample thickneses of 20A, 60A, 60A, and 110A respectively. The lines are drawn as guides to the eye.

3. The measured coercivities of three of the samples as a function of temperature. The sample thicknesses of 60A, 60A, and 110A correspond to the symbols block ■, cross ×, and square □ respectively. The lines drawn are guides to the eye.

4. The magnitude of the 5K loop shifts versus the inverse of the thickness.

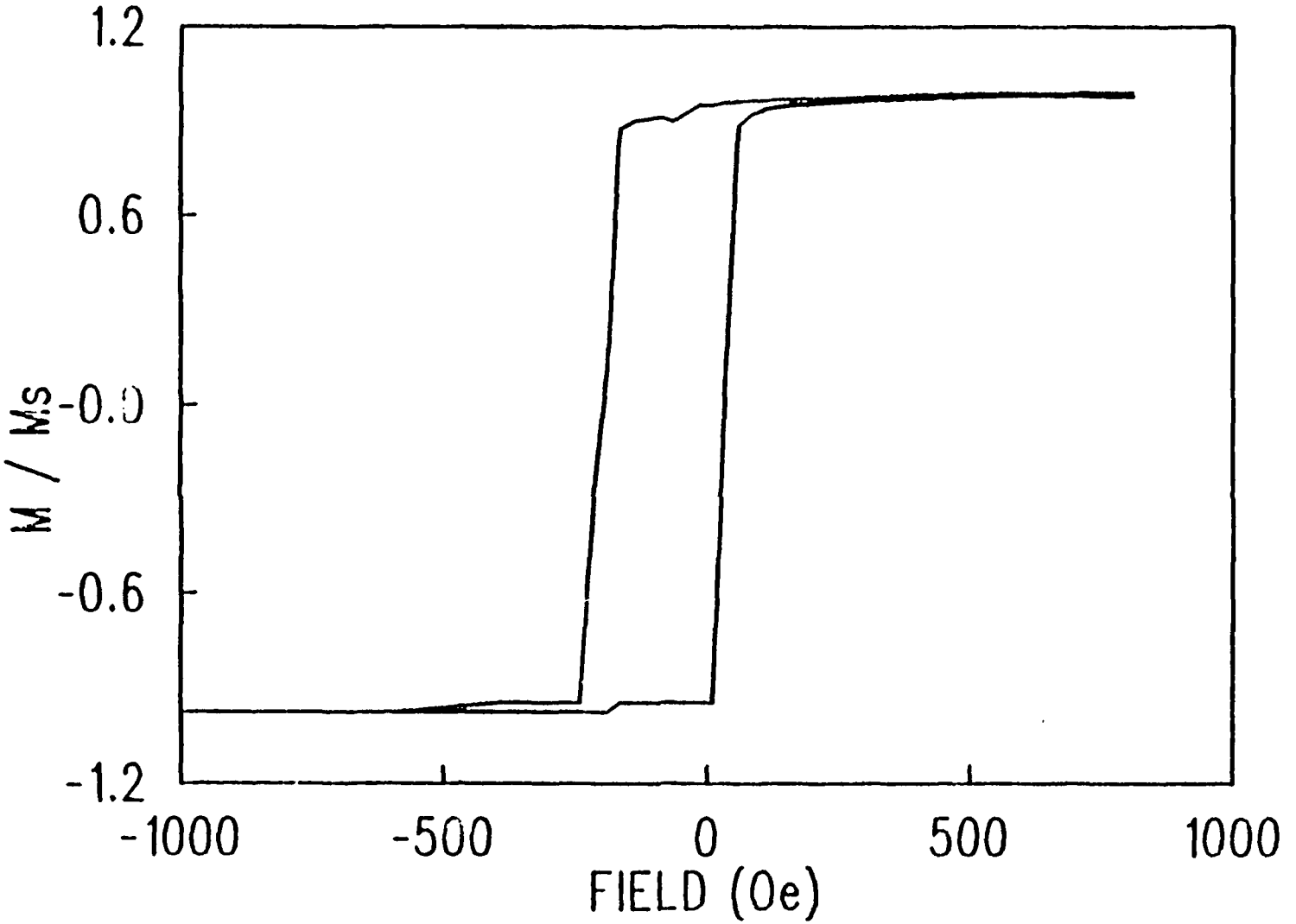
1.2
0.6
-0.0
-0.6
-1.2
M / Ms
-1000
-500
0
500
1000
FIELD (Oe)

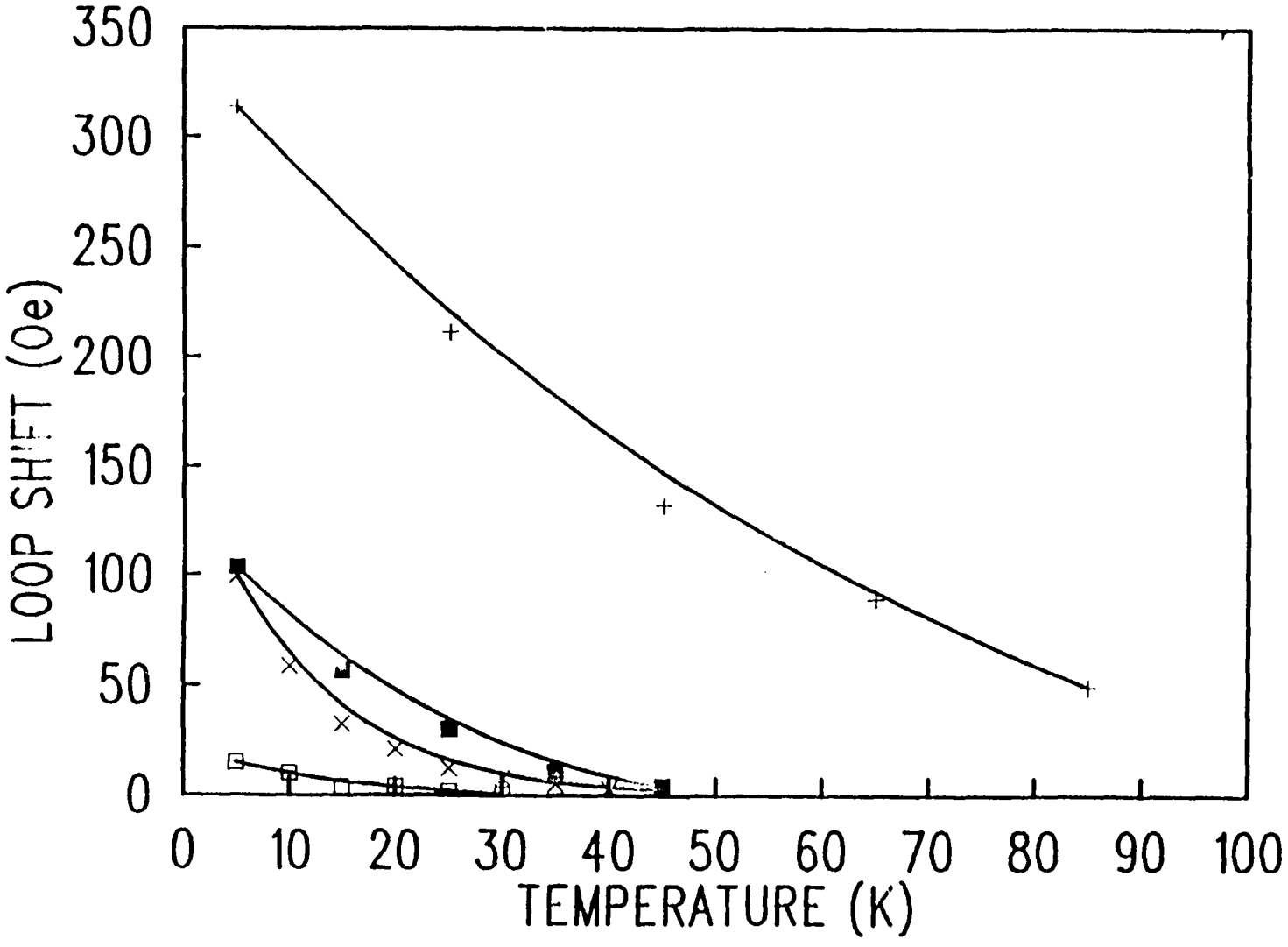
350
300
250
200
150
100
50
0
LOOP SHIFT (Oe)
0
10
20
30
40
50
60
70
80
90
100
TEMPERATURE (K)

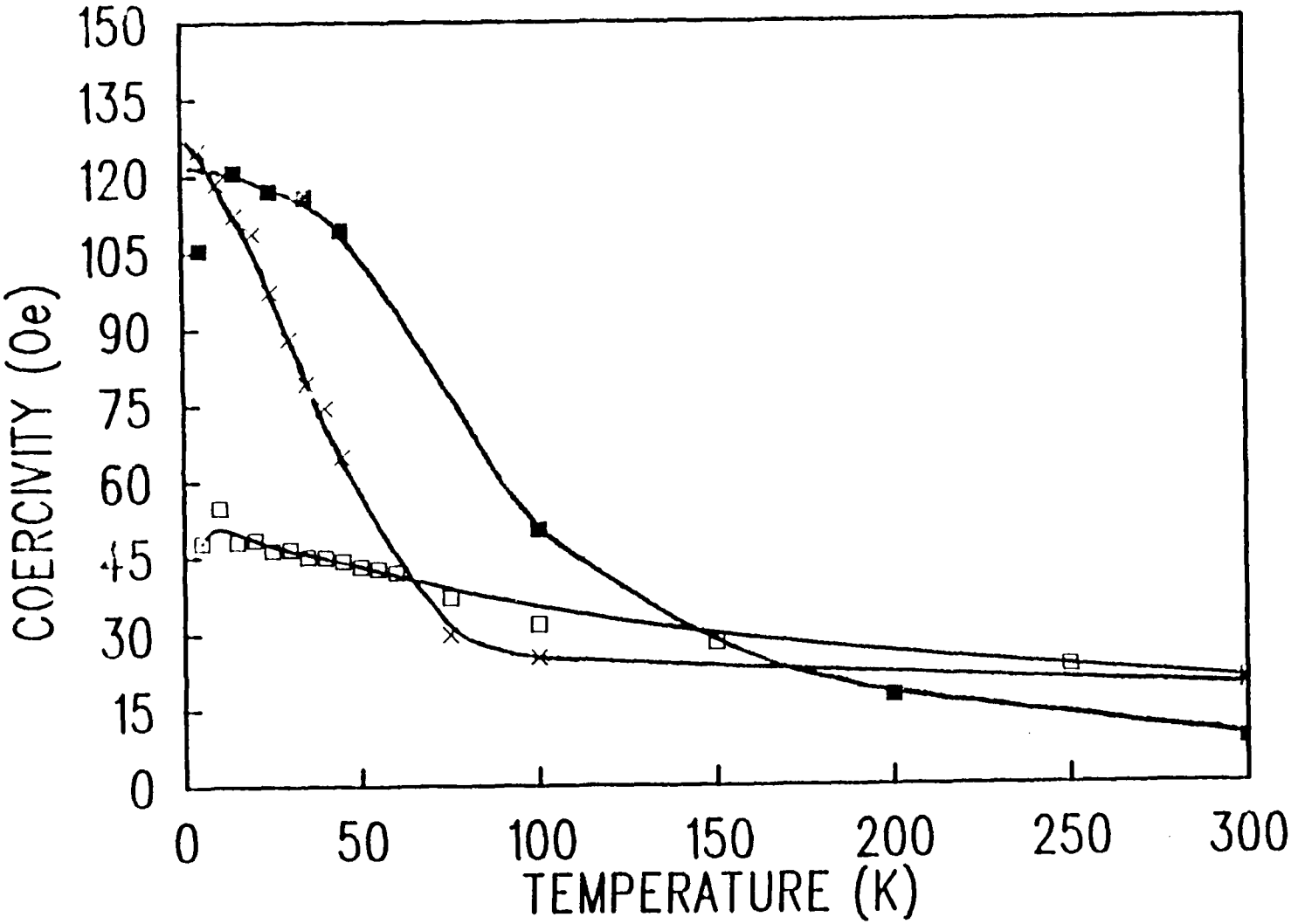
150
135
120
105
90
75
60
45
30
15
0
COERCIVITY (Oe)
0
50
100
150
200
250
300
TEMPERATURE (K)

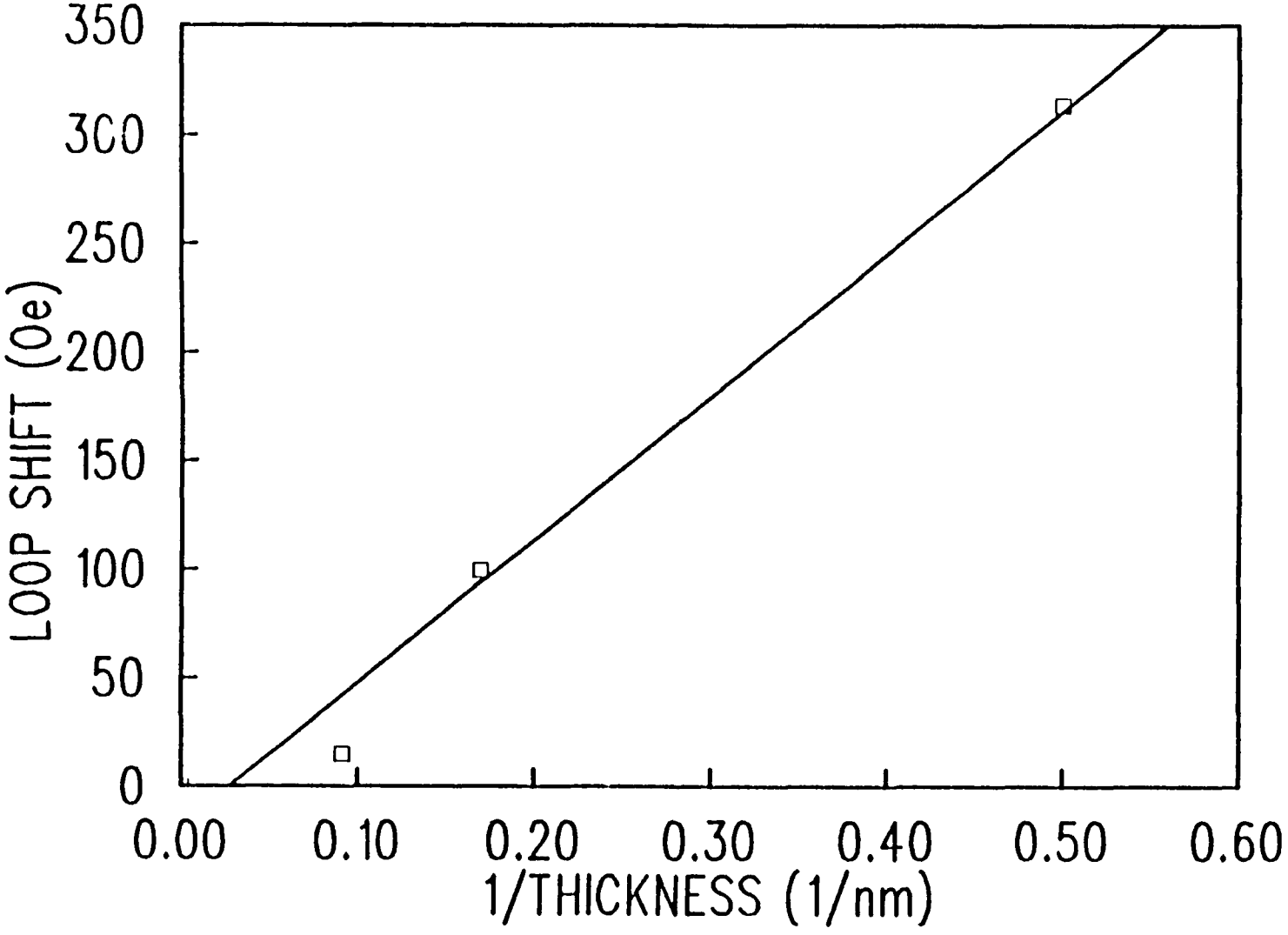
350
300
250
200
150
100
50
0
LOOP SHIFT (Oe)
0.00
0.10
0.20
0.30
0.40
0.50
0.60
1/THICKNESS (1/nm)

SIMULTANEOUS IN-PLANE KERR EFFECTS IN Fe/GaAs (110) THIN FILMS

J. M. Florczak and E. Dan Dahlberg
School of Physics and Astronomy, 116 Church St. S.E.
and
J. N. Kuznia, A. M. Wowchak, and P. I. Cohen
Department of Electrical Engineering
University of Minnesota, Minneapolis, Minnesota 55455

Abstract

For many materials that can be magnetized, part of the magnetization process may be attributed to a rotation of the magnetization vector. In this context, a combination of the longitudinal and transverse magneto-optical Kerr effects are used to detect two orthogonal magnetization components in single-crystal Fe/GaAs (110) thin films. Hysteresis curves obtained by this magneto-optical technique are presented for fields along the in-plane [001], [1$\bar{1}$0], and [1$\bar{1}$1] crystal directions. For those curves that show signs of rotation, these data are simulated using a coherent rotation mechanism for the magnetization process and Fresnel reflection coefficients for the two Kerr effects. From the experimental data, it is found that the [1$\bar{1}$1] curves have shapes that are indicative of a rotational process. On the other hand, both the [001] and [1$\bar{1}$0] have magnetization curves that do not follow a simple rotation. From the coherent rotation model, there is qualitative agreement between the modeled and experimental data for the [1$\bar{1}$1].

PACS numbers: 78.20.Ls, 75.60.Ej

Introduction

For ferromagnetic materials that magnetize partly by a rotation process, the best techniques for confirming this rotation utilize the vector nature of the magnetization. Within this context, the in-plane magneto-optical Kerr effects can be utilized to detect two orthogonal magnetization components.[1] This technique is used to investigate the magnetization processes in Fe/GaAs (110) thin films. These systems have been extensively studied by ferromagnetic resonance,[2,3] vibrating sample magnetometry (VSM),[4] and by magnetoresistance measurements.[5] The advantage of the (110) Fe films is that three high symmetry directions, the [001], [1$\bar{1}$0], and the [1$\bar{1}$1], are present in the plane of the film.

The motivation of this work is to use the magneto-optical technique to explore the rotational processes for applied fields along the [1$\bar{1}$0] and [1$\bar{1}$1]. Previous VSM data indicated that for these two orientations, the shapes of the magnetization curves were suggestive of a rotational process.[3] With the magneto-optical technique, it will be possible to track the direction of the magnetization vector during the rotation. Thus, for those directions that show definite signs of rotation, the reversal process can be

simulated with a coherent rotation model for the magnetization process and Fresnel coefficients for the dual Kerr effects. In this way, possible modes for the rotational process can be eliminated by a comparison of the modeled and experimental data.

Experimental

The films used in this study were prepared with current molecular beam epitaxy (MBE) techniques. The GaAs (110) substrate, misoriented by 1^{0} to the $[11\bar{1}]$, was etched in a standard 6:1:1 solution of $H_2SO_4:H_2O:H_2O_2$. The resulting surface oxides of the substrate were removed by heating to 620^{0}C in vacuum. A 700 $\overset{0}{A}$ GaAs buffer layer was then grown at 540^{0}C at a rate of 5sec/layer using a large As overpressure of $4x10^{-6}$ Torr. This large As overpressure was used to prevent Ga puddling. After allowing the pressure to fall to $3x10^{-9}$ Torr, 100 to 150$\overset{0}{A}$ of Fe were deposited at a substrate temperature of 200^{0}C. Subsequent RHEED measurements revealed good epitaxial growth of the Fe but a rather rough surface.

The magneto-optical measurements were made at room temperature using a HeNe laser at λ=6328$\overset{0}{A}$. The light incident upon the film was polarized in the plane of

incidence. The sample was mounted on a rotatable stage between the pole faces of a magnet in such a manner that the applied field was perpendicular to the plane of incidence formed by the incident and reflected light.

The detection of two magnetization components, individually or simultaneously, depends upon the analyzer orientation.[1] Basically, for analyzer angles near extinction, the component parallel to the plane of incidence is dominant while for angles 90^{o} from extinction, the component perpendicular to the plane of incidence is important. At angles intermediate between these two extremes, both components are simultaneously detected.

Results and Discussion

Depicted in Fig. 1 are the magnetization loops for an applied field along the [001], [1$\bar{1}$0], and [1$\bar{1}$1] with an analyzer angle of 45^{o} from extinction. The square magnetization curve for the [001] is indicative of the absence of any rotation beyond the transition at 250 Oe. This is implied by the constant intensity for applied fields in excess of 250 Oe. In contrast, the [1$\bar{1}$0] and [1$\bar{1}$1] have shapes that can be interpreted as a result of a rotation. To cross check this, one can monitor the component

perpendicular to the applied field. Fig. 2 portrays the magnetization curves for the same crystal directions but with the analyzer now rotated to within 5^{0} of extinction. Recall that for this orientation of the analyzer, the magnetization component parallel to the plane of incidence is sensed to a greater degree than that in Fig. 1. Considering these data, in addition to Fig. 1, it appears that a rotation process occurs only when the applied field is along the $[1\bar{1}1]$ and not in the other directions. These conclusions are deduced by the following considerations. Comparing figures 1a and 2a, and figures 1b and 2b, only the saturation to saturation intensity difference is altered, and this is due to the simple crossing of the polarizer and analyzer. A comparison of figures 1c and 2c indicate a qualitative difference in the shape of these hysteresis curves suggesting the presence of a component perpendicular to the applied field.

For the $[1\bar{1}1]$ curve, assuming the magnetization rotates toward the [001] as the applied field is reduced from 900 Oe, the component perpendicular to the applied field increases as the applied field decreases, as is suggested by the increasing intensity of the magnetization curve. At saturation, either at positive or negative 900 Oe, the magnetization lies parallel to the applied field resulting

in the absence of a component perpendicular to the applied field. This is the reason why the intensity is so similar at the two saturated states. On the other hand, for the [001] and [1$\bar{1}$0], only the small change due to the switching of the component parallel to the applied field is detected, no analyzer dependence of the shape of the curve is noted. This suggests that for these two directions, beyond the intial transition, a rotation of the magnetization is not present, at least to the sensitivity of this technique.

To model the magnetization curves, two ingredients are required: the intensity expression that relates the photodiode current to the direction of the magnetization and the polarizer/analyzer angles, and the magnetization process, in this case a coherent rotation model.

First, the photodiode current, which is proportional to the light intensity after the analyzer, can be shown to have the form[1]

$$I/I_0 = |m_l^2 r_{pp}^l + m_t^2 r_{pp}^t|^2 \cos^2\theta_a + |m_l^2 r_{ps}^l|^2 \sin^2\theta_a$$
$$-[(m_l^2 r_{pp}^l + m_t^2 r_{pp}^t) m_l^2 r_{ps}^{l*} + c.c.]\cos\theta_a \sin\theta_a, \qquad (1)$$

where θ_a is the analyzer angle measured relative to the plane of incidence, m_t and m_l are the components of the

magnetization perpendicular and parallel to the plane of incidence, and the terms of the form r_{ps}^{l} are the Fresnel reflection coeffients for the transverse or longitudinal Kerr effects.

Secondly, previous work by magnetoresistance[6] suggests that these systems can be modeled using a phenomenological expansion of the free energy density of the form

$$E = K_1(\alpha_1^2\alpha_2^2 + \alpha_1^2\alpha_3^2 + \alpha_2^2\alpha_3^2) + K_u\sin^2\theta + 2\pi M_n^2 - \vec{M}\cdot\vec{H}, \qquad (2)$$

where in this expression K_1 is the fourth order magnetocrystalline anisotropy with the α_i's being the direction cosines of $\vec{M}$ in a cubic system such as Fe, K_u is a uniaxial anisotropy with θ being the angle that $\vec{M}$ makes with the [001]; this term could be due to strain or preferential orientation of defects in the Fe film,[2,7] $2\pi M_n^2$ is the demagnetization energy for the component of $\vec{M}$ perpendicular to the film plane, and the last term is the energy of the magnetization in an applied field. By virtue of the large demagnetizing energy, the magnetization is effectively forced to lie in the film plane.

For a nonzero applied field, Eq. 2 is solved numerically for the stable orientation of the magnetization. The magnetization loop is the result of tracking the local energy minimum as a function of H. The components parallel and perpendicular to the plane of incidence can then be determined from the orientation of the magnetization. Simulations of the magnetization processes in Fe/GaAs (100) films by this method resulted in agreement with the data.[8]

Depicted in Fig. 3 is a comparison of the θ_a=85^0 for the simulated and experimental data. In the modeled magnetization curve, Fig. 3a, K_1/M_s=235 Oe, K_u/M_s=30 Oe, and the applied field is misoriented from the [1$\bar{1}$1] by 1^0 toward the [001]. This misorientation was used to induce a rotation in the assumed direction. These anisotropy constants that fit these data are in good agreement with those deduced by Riggs et al. for similar films.[6] The simulated curves have a good fit to the data.

For the film prepared here, the first order phase transition was not observed in the magnetization data for the [1$\bar{1}$0].[4,9] This could be a result of the surface roughness or the misorientation of the (110) GaAs toward a [11$\bar{1}$]. For the anisotropy constants specified by others,[5,9] the simulations here predict the general shape seen in the

VSM data,[4] including the discontinuities in the magnetization as a function of the applied field. However, the shape of the simulated curves are sensitive to the value of K_u. Thus, if the surface roughness or the misorientation of the (110) GaAs can induce a significant change in the value of K_u, the absence of the first order transition could be accounted for in this film. A small misorientation of the applied field from the $[1\bar{1}0]$ does not appear to be a plausible explanation since the discontinuity is still present even for misorientations of 7^{0}.[4] Another feasible explanation, given the large corercivity of this film along the [001] and the equivalent technical saturation field for the $[1\bar{1}0]$, is that the unpinning energy of the domains is comparable to the anisotropy energy resulting in a transition to the $[1\bar{1}0]$ without ever seeing the $[1\bar{1}1]$ energy maximum.

In summary, the magneto-optical technique indicates that the magnetization process for applied fields along the $[1\bar{1}1]$ is partly due a rotation process. The simulated curves reproduce the analyzer dependence seen in the data for the $[1\bar{1}1]$. However, the $[1\bar{1}0]$ magnetization curve does not show signs of a first order phase transition seen in

similarly prepared films. A possible explanation could be the presence of a rough surface or the misorientation of the substrate.

Acknowledgements

We wish to express our gratitude to the AFOSR for their support of this research under Grant No. AF/AFOSR-89-0248. One of us, J. Florczak, would like to thank IBM for their support under an IBM fellowship.

References

1.) J. M. Florczak and E. Dan Dahlberg, J. Appl. Phys. 67, 7520 (1990)

2.) J. J. Krebs, F. J. Rachford, P. Lubitz, and G. A. Prinz, J. Appl Phys. 53, 8058 (1982)

3.) G. A. Prinz, G. T. Kado, and J. J. Krebs, J. Appl. Phys. 53, 2087 (1982)

4.) Kristl B. Hathaway and Gary A. Prinz, Phys. Rev. Lett. 47, 1761 (1981)

5.) Mark Rubinstein, F. J. Rachford, W. W. Fuller, and G. A. Prinz, Phys. Rev. B 57, 8689 (1988)

6.) K. T. Riggs, E. Dan Dahlberg, and G. A. Prinz, Phys. Rev. B. 41, 7088 (1990)

7.) G. A. Prinz and J. J. Krebs, Appl. Phys. Lett. 39, 397 (1981)

8.) J. M. Florczak and E. Dan Dahlberg, to be submitted for publication.

9.) F. J. Rachford, G. A. Prinz, and J. J. Krebs, J. Appl. Phys. 53, 7966 (1982)

Figure Captions

Fig. 1 Magnetization curves for an applied field along the a.) [001], b.) $[1\bar{1}0]$, and c.) $[1\bar{1}1]$. The analyzer is oriented 45^{0} from the plane of incidence. The data is scaled to bring the saturation states of $I(-M_s)$ and $I(+M_s)$ to relative values of +1 and -1, respectively.

Fig. 2 Magnetization curves for an applied field along the a.) [001], b.) $[1\bar{1}0]$, and c.) $[1\bar{1}1]$ with the analyzer oriented 85^{0} from the plane of incidence. The curves are multiplied by a factor of 30 relative to those in Fig. 1.

Fig. 3 A comparison of the a.) simulated magnetization curves to the b.) experimental curves for the $[1\bar{1}1]$ for an analyzer angle of 85^{0} from the plane of incidence. For these simulations, K_1/M_s=235 Oe, K_u/M_s=30 Oe, and the applied field is oriented 1^{0} from the $[1\bar{1}1]$ toward the [001].

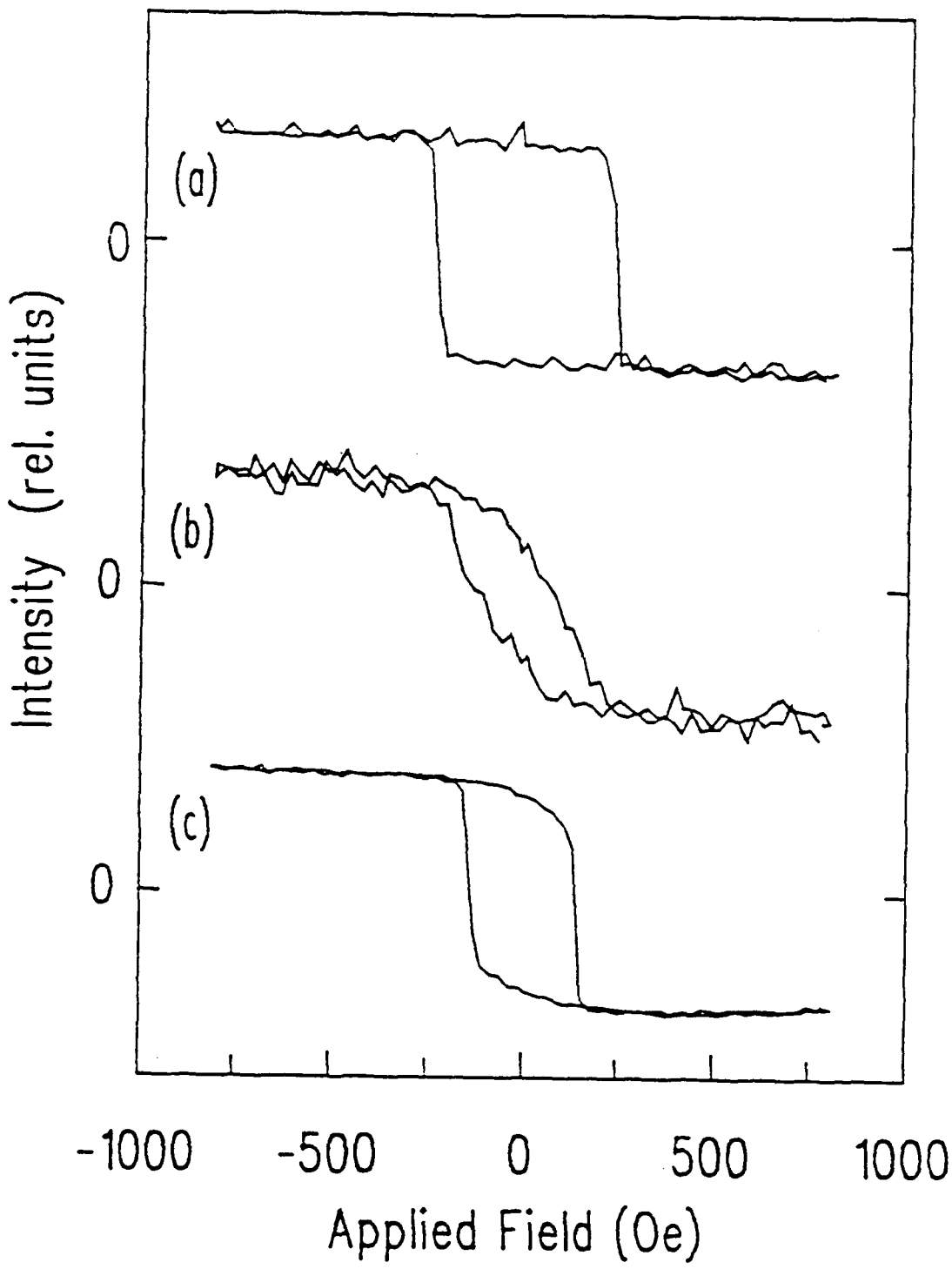
(a)
(b)
(c)
0
0
0
Intensity (rel. units)
-1000
-500
0
500
1000
Applied Field (Oe)

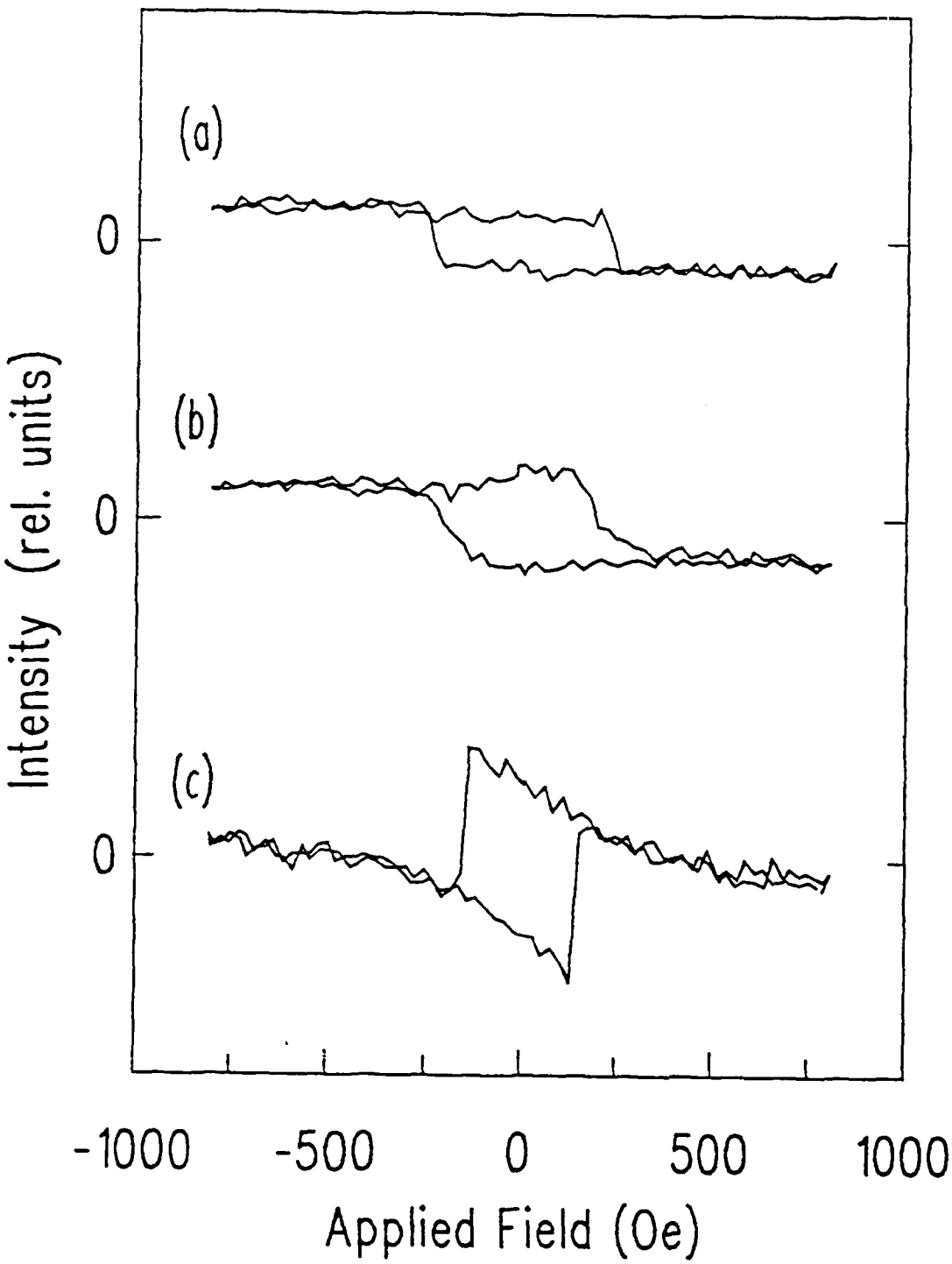
(a)
(b)
(c)
0
0
0
Intensity (rel. units)
-1000
-500
0
500
1000
Applied Field (Oe)

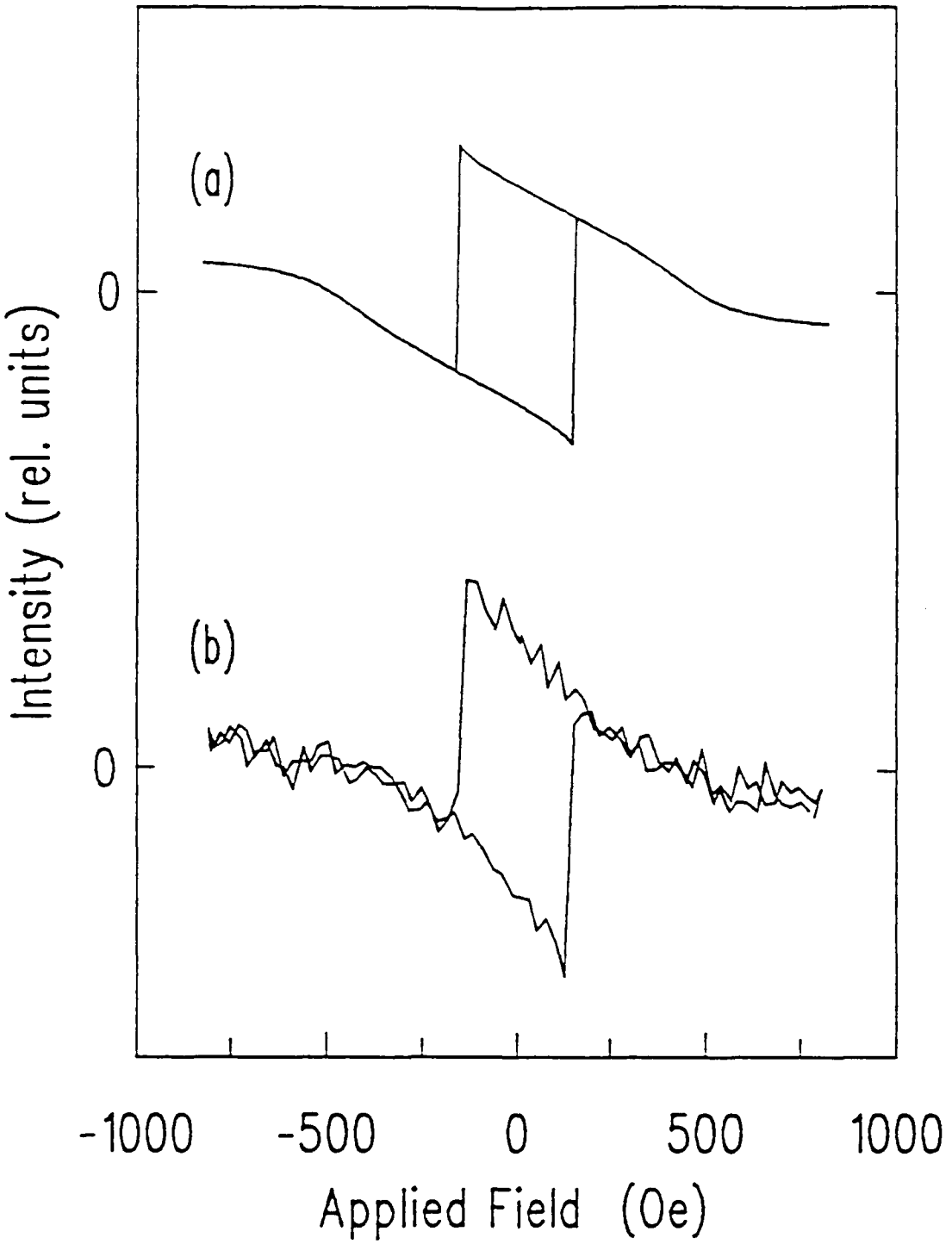
(a)
(b)
0
0
Intensity (rel. units)
-1000
-500
0
500
1000
Applied Field (Oe)

A Model System For Slow Dynamics

D.K. Lottis, R.M. White[+], and E. Dan Dahlberg[*]

School of Physics and Astronomy
University of Minnesota, Minneapolis, MN 55455

Abstract

Systems whose dynamics are described by a quasilogarithmic or stretched exponential time dependence are usually fitted by models which use disorder to create a distribution of relaxation times. Here we describe a model which decays slowly towards equilibrium but does not require disorder to provide the slow dynamic. The model is consists of a spin system with the spins interacting via the dipole-dipole interaction. The model is able to replicate the more pronounced features observed in the magnetization decay of magnetic systems and high temperature superconductors.

PACS numbers: 05.50.+q, 61.42.+h, 64.70.Pf, 75.10.Nr

+ Present address Department of Commerce, Washington, D.C. 20230

* Also at 3M Corporation, St. Paul, MN 55144-1000

A number of physical systems are known to relax more slowly than expected from a simple Debye relaxation model. These systems include glasses, polymers[1], and spin glasses.[2] Usually a distribution of relaxation times, a manifestation of disorder, is argued to be the origin of the slow relaxation of some property of the system[3]. Within the context of a distribution of relaxation times, the relaxing entities are noninteracting, i.e., the relaxation process occurs in parallel for all the entities. Using this generic model to analyze physical systems merely yields a distribution function describing the disorder which may or may not be identifiable with some physical property of the system. Similarly, computer simulations have also been plagued by their inability to make connections to real physical systems. Another theoretical approach has considered serial relaxation processes[4] rather than parallel relaxation. The model of heirarchially constrained dynamics that result from this approach do contain slow relaxation but are again phenomenological in nature.

In this letter we present a surprisingly simple model which requires no disorder to provide the slow relaxation observed in so many systems. In this model, interactions provide for the slow dynamic which are manifest by either quasilogarithmic or stretched exponential behavior. In particular the model predicts the nonmonotonic temperature dependence observed in the decay of the remanent magnetization of CoCr films[5] and high temperature superconductors.[6,7] Although not contained in the present paper, it may be used as a direct comparison of the dynamics generated by Monte Carlo calculations on spin systems.

The system consists of a planar array of spins with an anisotropy energy which is a minimum when the spins are perpendicular to the plane. The model includes the dipole-dipole interaction between the spins which are in essence, the causal agent of the slow relaxation. The interactions are treated in the mean field limit using the demagnetization field arrising from the plane of spins.

Due to the dipole-dipole interaction between the spins, the ground state possesses no net magnetization perpendicular to the plane even though the anisotropy energy for a single spin prohibits the spins from lying in the plane; the ground state is in effect an antiferromagnet. If the system is initially polarized with all the spins oriented perpendicular to the plane there will be a demagnetization field which drives the system to the ground state or the zero net magnetized state. Because of the anisotropy energy inhibiting the relaxation process and the fact that the drive field reduces as the system relaxes, there is a slow demagnetization of the spins. In what follows, we will outline the model, exhibit some of its interesting features, and discuss how it may pertain to a variety of other systems.

The fundamental unit of the model is a single magnetic entity such as a grain of a magnetic material which has a volume v, and a saturation magnetization of m_s. This grain, or spin as we refer to it, has a magnetic anisotropy of the form $-K_u\cos^2(\theta)$ where K_u is positive and θ is the angle between the magnetization vector and the +z axis. In the presence of an external field H, in the -z direction, the energy of the magnetic grain is given by

$$E = -K_u v \cos^2(\theta) + M_s H v \cos(\theta). \qquad (1)$$

This equation is the starting point for Neel's model[8] of fine grains used to model the temporal evolution the magnetization of the solidified magma in the earth's crust.

Of particular interest to the present discussion is to consider the relaxation of a number, N, of the above particles which lie in the x-y plane in a sheet one layer thick. The N particles or spins, as they will be refered to usually, are prepared in a state with the magnetization saturated in the +z direction. The process of reversing the magnetization of a particle requires the rotation of the magnetization past a energy barrier which is due to the anisotropy energy. In the presence of a reversed magnetic field (-z direction), one may determine the value of θ for the maximum value of the energy by differentiating eq.1 with respect to θ and setting the derivative equal to zero. Following this procedure one finds the energy maximum E_B, separating the +z and -z magnetic states to be given by

$$E_B=(m_s^2H^2v)/(4K_u). \qquad (2)$$

In order to determine the dynamics it is the energy differences between the up and down states relative to the energy maximum or barrier which are relevant. These energies are given by

$$E_{+(-)}=[v/(4K_u)](m_sH-(+)2K_u)^2 \qquad (3)$$

where the $E_{+(-)}$ refers to the energy difference between the up (down) state and the energy barrier. Using these energies, the rate equation is then given by

$$dn_+/dt = -w_+ n_+ e^{-\beta E+} + w_- n_- e^{-\beta E-}, \qquad (4)$$

where $n_{+\ (-)}$ is $N_{+\ (-)}$ is the number of antiparallel (parallel) divided by N, β is $1/k_B T$ and $w_{+(-)}$ is the attempt frequency from the up (down) state, antiparallel to the applied field, to the down (up) state. Expressions for the w's which depend upon the state of the system have been derived by Brown[9] and by Neel[10] but our calculations indicate that very little inaccuracy is induced by considering the w's to be equal and independent of the applied magnetic field.

If the decay of the magnetic system described by equation 4. is monitored at a fixed time eg. 30 sec, as a function of the applied magnetic field, one will find a maximum in the decay rate when the applied field is equal to $2K_u/m_s$, the coercive field for this model system. Physically this can be understood by realizing that this field corresponds to the disappearance of the energy barrier separating the up and down states. For fields less than this field, the energy barrier is too large to allow the magnetic moments to flip and the rate dn_+/dt is small. When the applied field is larger, most of the magnetization has flipped so dn_+/dt is small at the prescribed time. It is only when the applied field is equal to the coercive field that the decay rate from + to - is large.[11]

We now consider the modification to this model which provides for the slow dynamics; allow the spins to interact via the dipole-dipole interaction. As before, consider the N grains of the system to be confined to a plane with the easy direction of the magnetization of the grains to be perpendicular to the plane. In the mean field situation the dipole-dipole interaction is given by the demagnetization field of the plane of spins interacting with the grains. The demagnetization field is given by $4\pi M$ where M, the magnetization of the sample is given by $m_s(n_+ - n_-)$. By defining a δn such that $n_+ = 1/2 + \delta n/2$ and $n_- = 1/2 + \delta n/2$ then the demagnetization field is just $H_d = 4\pi m_s \delta n$.

If the planar sample of magnetic grains is first polarized with all the magnetization in the +z direction, then the demagnetization field is directed opposite the magnetization and will tend to drive the system into a demagnetized state. But as the magnetization of the system decays, the driving field or the demagnetizing field will also become smaller thereby reducing or slowing down the dynamics of the system. This is the essence of the origin of the quasilogarithmic decay of the magnetization of the system.

If the applied field in eq.3 is replaced by the demagnetizing field, the above definitions are used, and after a little algebra, then the rate of the decay of δn is given by

$$d\delta n/dt = -w_+(1/2+\delta n/2)\exp\{(-\beta v K_u)[(2\pi M_s^2 \delta n/K_u)-1]^2\}+$$

$$w_-(1/2-\delta n/2)\exp\{(-\beta v K_u)[(2\pi M_s^2 \delta n/K_u)+1]^2\}. \qquad (5)$$

Again for this situation we should note that one may derive relationships for the w's but in solutions of eq.5 little difference is exhibited if the w's are equal and constant. Equation 5 describes the relaxation of a system of

particles where the drive force for the relaxation depends upon the instantaneous state of the system. As stated earlier, this expression is in the mean field limit and does not consider the actual discreteness of the relaxing grains nor their particular geometry. This expression is amenable to numerical techniques for its solution with different values of the parameters in the expression. Figure 1 shows an example of eq.5 solved using a Runge-Kutta algorithm[12] and indicates that the relaxation is quasilogrithmic over 7 decades in time! The recovery of a simple Debye relaxation of this model is accomplished when the argument of the exponentials are less than unity which occurs when the magnetic entities are in the superparamagnetic limit. A useful or effective approximation to this limit is $\beta > vK_u$; this is the usual condition for the superparamagnetic limit.

Two systems which would appear to be ideally modeled by the above are saturated films of CoCr[13] which have a perpendicular anisotropy and superconductors which have been cooled in a magnetic field trapping flux. In both cases the systems are out of equilibrium possessing a net magnetization thereby providing a decaying driving force. Also, their dynamics may be described by incremental changes in the magnetic state, i.e., for the CoCr films the magnetization in a single grain flips its magnetization direction, and in the superconductor a flux quantum leaks out of the sample.

In the case of CoCr films, the morphology of the alloy consists of small columnar grains of a magnetic alloy imbedded in a nonmagnetic matrix.[14] The column axes of the grains are perpendicular to the plane of the film and define the magnetically easy direction for the magnetic moment of the grains. In the superconductor case, it is again the remanent magnetization which is describable by the above model.[6] When the magnetic field is removed, the

superconductor will generally maintain some density of vortices pinned by defects which gives a situation analogous to the magnetic grains discussed above. The pinning energies play the role of the anisotropy energy in the magnetic film.

We should point out one rather strong similarity of the two systems and their remanence decay. All the simple models which give a slow decay, either logarithmic or quasilogrithic, also predict a monotonic increase in the decay rate with increasing temperature. In CoCr films and in high temperature superconducting samples the experimental evidence is contrary to this prediction; in both cases the decay rate passes through a maximum value with increasing temperature.

The model presented also contains such behavior. At low temperatures the remanent magnetization is large but because there is little thermal energy the decay slope is small. At very high temperatures the thermal energy is sufficient for the system to relax rapidly but in the time window of the measurement most of the magnetization has decayed and therefore the decay slope is reduced. This is very similar to the rationale of why there is a peak in the decay rate at the coercive field in the Neel model described previously. This nonmonotonic behavior is shown in the inset of fig.1.

One should note that the argument of the exponential in Eq. 5 is quadratic in the decaying variable. This arises from the way the applied field determines the θ for the maximum energy. In a different system which does not behave in this manner, the argument of the exponential may be linear. In this case eq 5, again gives a function which decays quasilogarithmically for long times. The linear form may be more relevant for systems where the free energy provides the driving force i.e., the argument of the exponential

is of the form dF/k_BT where dF is the difference in free energy of the instantaneous configuration from equilibrium.

For application to other systems, such as glasses, one may object to the use of a mean field approximation. In the case of structural glasses the strain fields are long range falling off as $1/r^3$ just as the dipole-dipole interaction; therefore a mean field approximation should be applicable. In the case of spin glasses the dipole-dipole interaction is expected to play an important role just as in the magnetic model presented here.

A final point to make is the connection between the present model and that of the theoretical model which generates a stretched exponential[4] via a hierarchy of constraints. In that paper, with certain approximations, is derived a stretched exponential relaxation of the form

$$M(t)=M_0\exp[-(t/\tau)^{\beta}], \qquad 0<\beta<1. \tag{6}$$

As argued, this form of relaxation is often observed in strongly interacting systems. Within the present model, we have been unable to fit this form of the relaxation over the entire time domain of the relaxation process, but do find our model can be approximated by the stretched exponential form over several decades in time, as shown in figure 2. This is the same data as exhibited in figure 1 but plotted in a magnetization domain where the stretched exponential form applies. In the plot as shown, a stretched exponential decay should be a straight line. The question as to whether or not the stretched exponential form should be applicable for all times in a real physical system remains open, but in at least spin glasses it does not appear to hold. Consequently, the fact that our model can only be fitted by a

stretched exponential over a limited time domain is not a serious deficit of the model.

Acknowledgements

One of the authors (EDD) would like to thank Professors J. Kakalios, L. Glazman, G. Mazenko, O. Valls, and B. Shklovskii for a number of interesting discussions. This research was supported in part by AFOSR grant AFOSR-89-0248.

References

1.K.L. Ngai, Comments Solid State Phys. 9, 127 (1979), and 9, 141 (1979).

2.O.S. Lutes and J.L. Schmidt, Phys. Rev. 125, 433 (1961) and Y. Ishikawa, R. Tournier, and J. Philippi, J. Phys. Chem. Solids 26, 1727 (1965).

3.J.J. Prejean and J. Souletie, J. de Physique 41, 1335 (1980).

4.R.G. Palme D.L. Stein, E. Abrahams, and P.W. Anderson, Phys. Rev. Lett. 53, 958 (1984).

5.D.K. Lottis, E. Dan Dahlberg, J.A. Christner, J.I. Lee, R L. Peterson, and R.M. White, Jour. de Phys. 49, C8-1989 (1989).

6.M. Tuomenen, A.M. Goldman, and M.L. Mecartney, Phys. Rev B37, 548 (1988).

7.C.W. Hagen and R. Griessen, Phys. Rev. Lett. 62, 2857 (1989).

8.L. Neel, Rev. Mod. Phys. 25, 293 (1953) and Chikazumi "Physics of Magnetism" (Wiley, New York, 1972) Chapter 15.

9. William Fuller Brown, Jr., Jour. Appl. Phys. 30, 130S (1959).

10. L. Neel, Compt. Rend. 228, 99 (1949).

11. One should note that the data are taken in a fixed time window. Assuming that the relaxation of the system is not to fast nor to slow allows the peak to be at the coercive field. Although it would appear that the window restriction would invalidate the analysis, in practice, as long as one is in a temperature limit where a slow dynamic is observed, it is a reasonable assumption.

12. W.H. Press, B.P. Flannery, S.A. Teukolsky, and W.T. Vetterling, "Numerical Recipes," (Cambridge University Press, New York, 1986) pp. 550-554.

13. D.K. Lottis, R.M. White, and E. Dan Dahlberg, submitted for consideration of publication.

14. M.R. Kahn, J.I. Lee, D.J. Seagle, and N.C. Fernelius, Jour. Appl. Phys. 63, 833 (1988).

Figure 1.

An example of a slow decay of the model system given by equation 5. For this decay the relevant parameters are $K_u=5x10^5$ ergs, $M_s=200$ emu/cm^3, T= 300K, $v=2x10^{-18}$, and $w_+=w_-=2x10^4$ sec^{-1}. Note that the decay is measured over nine decades in time. The insert in the figure is the temperature dependence of the logarithmic slope of the decay taken at a time of 100 sec.. The nonmonotonic behavior of the slope is observed in magnetic and superconducting systems (see refs. 5,6 and 7).

Figure 2.

This is the data from figure 1 plotted to show its compatibility with a stretched exponential relaxation model. As shown, the stretched exponential is well described by this system for over 4 decades in time.

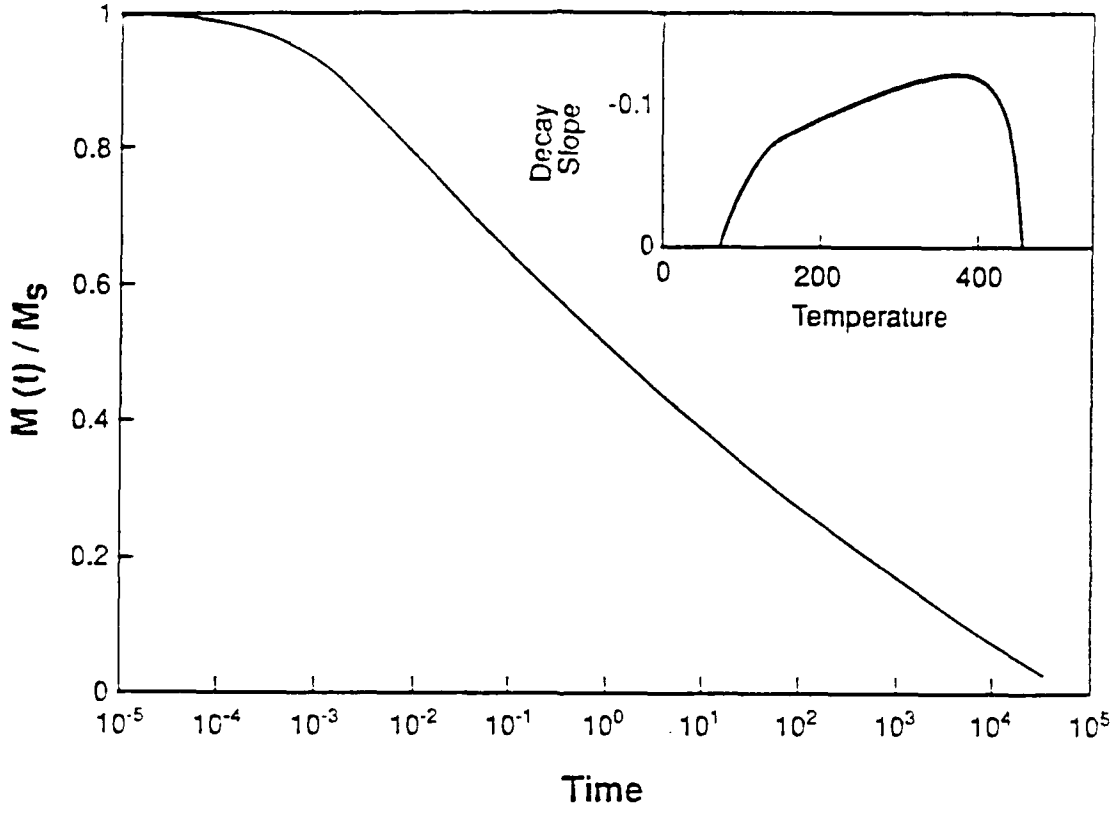
1
0.8
0.6
0.4
0.2
0
M (I) / Ms
10-5
10-4
10-3
10-2
10-1
100
101
102
103
104
105
Time
Decay Slope
-0.1
0
0
200
400
Temperature

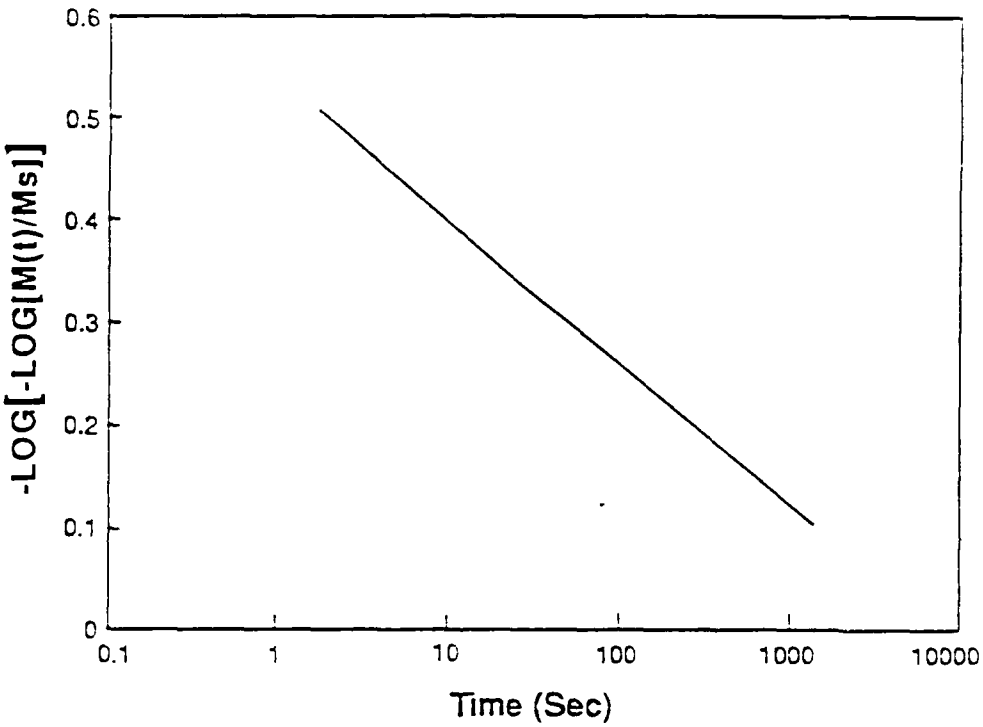
0.6
0.5
0.4
0.3
0.2
0.1
0
-LOG[-LOG[M(t)/Ms]]
0.1
1
10
100
1000
10000
Time (Sec)